Glowing Gems: Fluorescence and Phosphorescence of Diamonds, Colored Stones, and Pearls

Ulrika F.S. D'Haenens-Johansson, Sally Eaton-Magaña, W. Henry Towbin, and Elina Myagkaya

The use of photoluminescence imaging for gemstone characterization is reviewed, considering both fluorescence and its time-delayed counterpart, phosphorescence. Luminescence results from the excitation of atomic impurities and defects by an external source. Fluorescence can be excited by ultraviolet, visible, or infrared light, or even X-rays. Fluorescence to long-wave UV light is a characteristic included in diamond grading reports issued by major gemological laboratories. This article provides a comprehensive overview of the principles, mechanisms, and characteristics of luminescence that create the impressive and memorable glow of gemstones. Although diamond is the focus, a variety of colored stones and pearls are reviewed as well. This article is intended to foster a deeper appreciation of the complexity necessary to understand these natural wonders.

Have you ever wondered why certain materials appear to glow from within when exposed to ultraviolet light? Luminescence, the emission of energy as light following the absorption of applied energy, is a fascinating and often beautiful property of many minerals and gemstones (figure 1). Luminescence phenomena can be classified according to the excitation source, such as: incident light or photons (photoluminescence, PL), an electron beam (cathodoluminescence), heat (thermoluminescence), electric currents (electroluminescence), and friction (triboluminescence). Luminescence signals can be detected through visual inspection, camera imaging, or spectroscopic means. This review will focus on photoluminescence, further separated into fluorescence or phosphorescence (within gemology defined as during or following excitation, respectively), as well as observations and imaging as routes to explore luminescent defects in gem materials. The luminescence energies or wavelengths (which are inversely proportional to one another) of a suitably excited gemstone can reveal a wealth of information related to its chemical and structural identity and purity. Additionally, the spatial distribution of luminescence features can elucidate a gem's unique growth and potential treatment history. Although applications for colored stones and pearls will be discussed, diamond will be the primary example presented. The detailed multidisciplinary study of diamond's luminescence has captivated gemologists, geologists, and physicists for centuries since Robert Boyle's first reported observation in 1664 (Boyle, 1664).

In Brief

- Ultraviolet light can excite fluorescence and phosphorescence in many gems, providing insights into the material's chemical and structural identity.
- The luminescence response depends on the excitation wavelength. Deep-UV illumination (<225 nm) will induce fluorescence from practically all diamonds, even if inert to long- or short-wave UV.
- The luminescence colors observed depend on the impurity and structural defect structures present in the crystal lattice.
- The spatial distribution of luminescence features can reveal whether a gem is natural or laboratory-grown, and may also indicate treatment, coating, dyeing, and fracture filling.

See end of article for About the Authors and Acknowledgments.
Gems & Gemology, Vol. 60, No. 4, pp. 560–580,
http://dx.doi.org/10.5741/GEMS.60.4.560

Figure 1. Burmese ruby and diamond necklace and earrings under daylight-equivalent (left) and long-wave ultraviolet (right, ~365 nm) illumination, revealing an alluring fluorescence response. Several of the diamonds show blue fluorescence attributed to the N3 (N_3V^0) defect, whereas trivalent chromium ions (Cr^{3+}) produce red fluorescence in the rubies. Intense red fluorescence is particularly common in Burmese rubies, though not exclusive to them (Webster, 1975; Fritsch and Waychunas, 1994). Courtesy of a private collector and Mona Lee Nesseth, Custom Estate Jewels. Photos by Robert Weldon.

PRINCIPLES OF LUMINESCENCE

A deeper understanding and appreciation of luminescence requires the consideration of the electronic states of the species within a material being excited (e.g., a structural defect or impurity) and where they lie relative to the electronic band structure of the crystal. The electronic band structure of a solid describes the energy ranges or levels that its electrons may have according to the principles of quantum mechanics. This model lays the foundation for explaining many of the electronic and optical properties of insulating and semiconducting materials such as gemstones.

Diamond, for instance, consists of carbon atoms in a tetrahedral configuration, with each atom covalently bonded to four neighboring atoms. The interaction between the carbon atoms results in diamond's characteristic electronic band structure, illustrated in figure 2. The outermost electrons of the carbon atoms that are involved in the chemical bonding occupy the valence band, which is separated from the empty, electronically allowed conduction band by the forbidden band gap, with energy E_g. Diamond is classified as either an insulator or a wide-band gap semiconductor with an indirect band gap energy E_g ~5.49 eV (Clark et al., 1964)—practically too wide to conduct through thermal energy alone. However, if an electron in a perfect defect-free diamond is exposed to light with energy $>E_g$, the electron-pair bonds can be successfully broken and the electron can be excited into the conduction band, resulting in intrinsic edge absorption (Collins, 1992, 1993; Green et al., 2022). The excited electron leaves behind a hole in the valence band, conceptually a positively charged electron void. Together, the electron-hole pair is known as an exciton and can move through the crystal as a unit. As the electron deexcites back to the valence band, it releases energy in the form of a photon—i.e., creating luminescence and recombining with the hole. Since diamond is an indirect semiconductor, the excitation of electrons into the lowest energy level of the conduction band also involves lattice vibrational waves known as phonons, that are affected by the sample's temperature (Collins et al., 1990a; Collins, 1993; Barjon, 2017). The loss of energy through nonradiative processes means that the

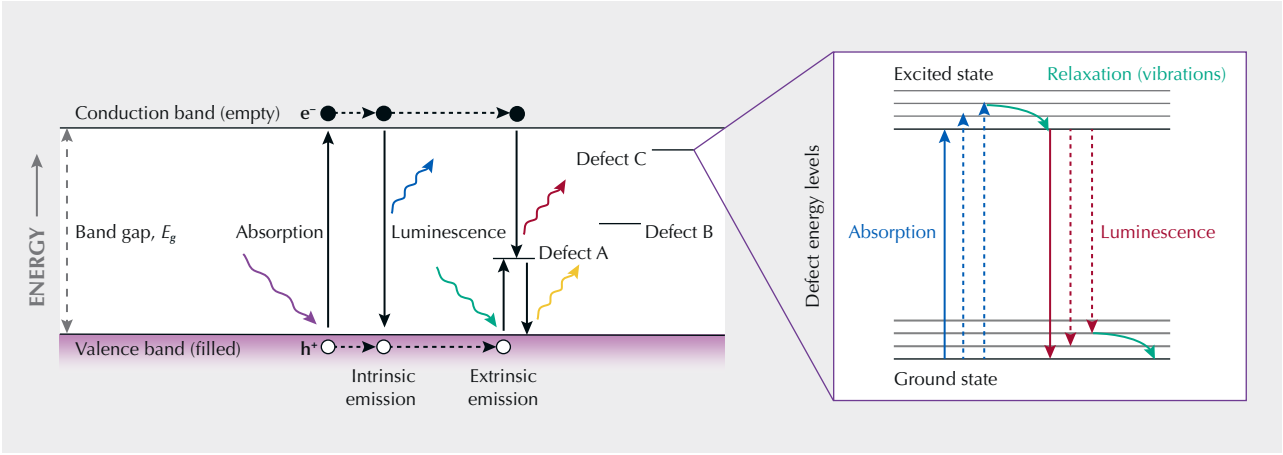

Figure 2. The filled valence band and empty conduction band in a semiconductor and insulator are separated by the band gap energy (E_g). Intrinsic luminescence can occur when incident photons (light) or electrons of energies greater than the band gap excite valence electrons (e^-) into the conduction band, leaving behind holes (h^+). In the absence of any defects, the electrons and holes may recombine, emitting intrinsic luminescence. Defects introduce energy levels within the band gap that can trap the electrons, resulting in extrinsic emission. Each defect has its own characteristic energy level structure that can also lead to absorption and emission processes at lower excitation energies. Nonradiative relaxation processes can also occur, producing vibronic structure in both the absorption and emission spectra (e.g., figure 3).

emitted light has a lower energy E (i.e., longer wavelength λ) than the light that was originally absorbed. In this ideal, defect-free diamond, the resulting emitted light is its intrinsic edge emission (Collins, 1992, 1993; Barjon, 2017).

Luminescence becomes significantly more interesting—and informative—if we move away from a perfect crystal. Crystalline gems can contain a variety of atomic-scale irregularities, scientifically termed *point defects*, in their crystal lattice due to their unique formation and post-growth environmental histories. For diamond, these point defects include missing carbon atoms (vacancies), displaced atoms (interstitials), and impurity complexes based on elements including nitrogen, boron, nickel, silicon, and hydrogen. Extended defects such as dislocations also exist. Their presence disturbs the host lattice, introducing additional energy levels within the band gap (figure 2). Defects introduce alternative relaxation pathways following exposure to above band gap excitation energies, leading to extrinsic emission with characteristic energies that allow the defects to be identified. Furthermore, these defects open up the possibility that incident light with energies smaller than the band gap energy (longer wavelengths) may be absorbed and subsequently emitted if the photon energy lies within a defect's absorption band. Thus, diamonds with defects can support vibronic transitions of electrons—combining vibrational and electronic interactions—between the valence band, defect energy levels, and the conduction band, leading to a rich combination of absorption and luminescence features (Collins, 1992, 1993).

In colored stones such as rubies, sapphires, and emeralds, it is the electrons in trace amounts of the metallic ions (e.g., Cr^{3+}, V^{3+}, and/or $Mn^{3+/2+}$) or rare earth elements in the host lattice that are excited and subsequently luminesce (Fritsch and Waychunas, 1994; Ponahlo, 2000; Waychunas and Kempe, 2024). These are often called activators. In some cases, sensitizers or coactivators, such as Pb^{2+} for Mn^{2+}, facilitate fluorescence by strongly absorbing the incident light and transferring the energy to the activator. Waychunas and Kempe (2024) present a detailed review of activators, sensitizers, and electronic defects and their roles in the luminescence of minerals.

The spectroscopic signatures of these luminescence features for diamond and other gemstones have been tabulated and described in several publications (e.g., Collins, 1982, 1992; Ponahlo, 2000; Zaitsev, 2001; Gaft and Panczer, 2013; Luo and Breeding, 2013; Shigley and Breeding, 2013; Gaft et al., 2015; Green et al., 2022; Zhang and Shen, 2023). Identifying the structural defects associated with these features is a nontrivial matter that combines rigorous experimental and theoretical work that may span several decades. Importantly, *correlation does not imply causation*. Somewhat confusingly, features may be referred to by their most recognizable energy or wavelength of absorption or emission

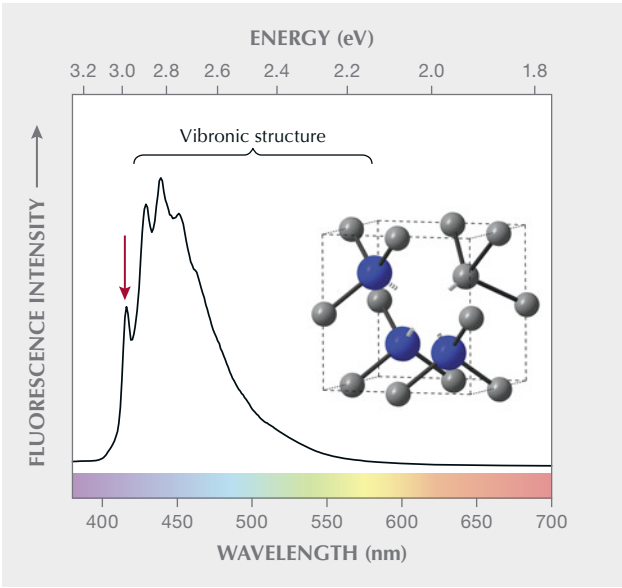

Figure 3. The blue fluorescence commonly observed for natural diamonds (e.g., figure 1) is attributed to emission from the N3 defect (inset), consisting of three nitrogen atoms surrounding a vacancy, N_3V^0. Its characteristic spectrum has a zero-phonon line at 415 nm (arrow) and vibronic structure extending to longer wavelengths.

(often the zero-phonon line [ZPL] for vibronic defects), by a nickname, or by their structural identity (if determined). For example, blue luminescence from diamond is often associated with the N3 defect (as pictured in figure 1) (Clark et al., 1956). It is characterized by a ZPL at 415 nm (2.985 eV), with vibronic structure extending to higher or lower wavelengths for emission and absorption, respectively (e.g., Davies et al., 1978). During room temperature luminescence, the vibronic structure of N3—peaking at ~450 nm—dominates (figure 3), resulting in visible blue emission. The N3 defect has been conclusively identified as three nitrogen atoms surrounding a vacancy, N_3V^0 (when considering diamond defects, "V" stands for a vacancy instead of the element vanadium) (Davies et al., 1978; van Wyk and Loubser, 1993; Green et al., 2017).

When multiple luminescing defect species are present, they may be excited simultaneously, depending on the incident energy. For energies above the band gap ($>E_g$), emission at defects can be induced by the capture of the exciton. Spectroscopically, each defect's contribution can be distinguished. Yet during visual or imaging-based observations, the overlapping luminescence features cannot be separated and instead the combined color is perceived. These contributions can be separated by optical filtering of the emission signal. Deliberate tuning of the excitation energy can also lead to selective excitation of defects, depending on their energy structure and absorption. If the incident energy of the photons ($<E_g$) matches the absorption spectrum of one or more defects, electron excitation may occur at those defects, followed by emission. If the energy does *not* coincide with the absorption of one or more of the defect species, those defects will remain inert and the overall luminescence response will instead be based on that of the other defects present.

Whereas the absorption of light by a defect is proportional to its concentration, the potential presence of other nonradiative relaxation pathways means that luminescence is only semiquantitative. A sufficient concentration of the defect must be present for significant absorption of the incident radiation, yet the subsequent emission may be weak if the energy is instead transferred nonradiatively to another defect, effectively quenching the defect's luminescence. For instance, the luminescence of N3 (N_3V^0), H3 (N_2V^0), and GR1 (V^0) defects in diamond can be quenched by A-centers (nitrogen pairs) (Davies and Crossfield, 1973; Crossfield et al., 1974; Thomaz and Davies, 1978; Davies et al., 1987), while the transition metal ions Fe^{+3}, Fe^{+2}, Co^{+2}, and Ni^{+2} are common quenchers in colored stones (Ponahlo, 2000; Fritsch and Waychunas, 1994; Yu and Clarke, 2002; Waychunas, 2014; Waychunas and Kempe, 2024). Other forms of quenching are concentration quenching, where high concentrations of activators in colored stones result in the fluorescence being absorbed by neighboring ions of the same species, and thermal quenching, where a temperature increase results in increasing lattice vibrations that carry off the excitation energy (Fritsch and Waychunas, 1994).

EVOLUTION OF FLUORESCENCE AND PHOSPHORESCENCE OBSERVATION METHODS

In 1852, the Irish physicist George Stokes created the term "fluorescence" to refer to the visible light reaction seen in objects when illuminated by ultraviolet light. In his magnum opus (Stokes, 1852), he added a footnote: "I am almost inclined to coin a word and call the appearance fluorescence, from fluor-spar [fluorite], as the analogous term opalescence is derived from the name of a mineral." The excitation ranges associated with the term have expanded over time to encompass short-lived luminescence excited by electromagnetic radiation from X-rays, ultraviolet, visi-

ble, and infrared sources. This feature is commonly observed in gemstones and minerals, and its measurement has become standard practice in gemology.

Gemologists typically observe fluorescence using long-wave (defined as 365 nm emission) and short-wave (254 nm) UV excitations, based on the filtered output from readily available and inexpensive mercury-vapor discharge lamps. Unfortunately, the band-pass filters in these portable lights deteriorate over time, allowing additional mercury emissions to slip through and leading to variability in the observed fluorescence (Williams, 2007; Pearson, 2011; Luo and Breeding, 2013). Filtering or monochromating the broadband emission of a xenon arc lamp is also an option (e.g., Hainschwang et al., 2013). Currently, long- and short-wave UV light is frequently produced for fluorescence applications using LEDs, or light-emitting diodes (Luo and Breeding, 2013).

In 1996, De Beers launched the DiamondView instrument, which illuminates samples using ultra-short wave or deep-UV illumination ($\lambda < 225$ nm, $E > 5.51$ eV) generated by filtering the output from a xenon flash lamp (Welbourn et al., 1996). Targeting diamond, this wavelength results in excitation with above band gap energy, inducing fluorescence from practically all diamonds, including those that are inert to long-wave and short-wave UV. As diamond is strongly absorbing of light with $E > E_g$, the fluorescence is generated close to the sample surface, resulting in sharp patterns that can be used as evidence of the diamond's identity (natural or laboratory-grown), as well as possible dissolution and treatment, as described later in this article. In a fully enclosed system, digital images of sample fluorescence and phosphorescence can be collected under either optical or digital magnification (original and current design, respectively). A selection of optical filters (blue = 390 nm band-pass, green = 475 nm long-pass, orange = 550 nm long-pass, and red = 725 nm long-pass) can be placed in the detection path to restrict the detected wavelengths, enabling more detailed inspection of the spatial distribution of otherwise overlapping emissions. The DiamondView rapidly established itself as a popular tool for diamond identification, and images collected from it are frequently included in diamond studies. Deep-UV fluorescence imaging studies of other gemstone materials are limited, though this energy can effectively excite common fluorescence features and provide the magnification necessary to observe their distribution.

UV lamp output can significantly affect the observed fluorescence and phosphorescence color and intensities for gemstones. Pearson (2011) and Luo and Breeding (2013) present emission spectra for common UV light sources used by the jewelry industry and hobbyists. Observation, whether unaided or using a microscope, should include light filtration through appropriate engineering controls and/or the use of UV goggles to avoid eye and skin damage. Color cameras can be used to safely capture and store fluorescence and phosphorescence images for subsequent analysis. Although most fluorescence testing in gemology today is still based on visual observation and imaging, technological developments and lower equipment costs have made fluorescence spectroscopy a much more widely used tool for rapid analysis (e.g., Hainschwang et al., 2013, 2024; Tsai and D'Haenens-Johansson, 2021; Zhang and Shen, 2023; Tsai et al., 2024).

There have been several compilations of fluorescence and phosphorescence observations across various gems (e.g., Kunz and Baskerville, 1903; De Ment, 1949; Webster, 1983; Fritsch and Waychunas, 1994; Hainschwang et al., 2024). These works established the definitions of fluorescence and phosphorescence still used by gemologists today. Namely, fluorescence is "luminescence lasting only during the direct influence of the exciting agent," and phosphorescence is the "emission or propagation of ethereal stresses, which affect the optical centers, producing light, white or colored, which persists after the removal of the cause" (Kunz and Baskerville, 1903).

FLUORESCENCE AND PHOSPHORESCENCE OBSERVATIONS OF DIAMONDS

Short-Wave and Long-Wave UV Excited Luminescence of Diamonds. The luminescence of diamonds has long captured the interest of the scientific community and the jewelry industry. One of the first documented instances was by the famous Irish scientist Robert Boyle, who noted that a flash of light was released when a diamond broke, a phenomenon now known as triboluminescence (Boyle, 1664). In 1813, the English mineralogist John Mawe discussed the luminescence of diamonds exposed to sunlight and also to electricity (electroluminescence) (Mawe, 1813). Since then, numerous publications have documented observations of fluorescence and, less commonly, phosphorescence in gem diamond (e.g., Anderson, 1943; Dyer and Matthews, 1958; Moses et al., 1997; Eaton-Magaña et al., 2007; Luo and Breeding, 2013; Breeding and Eaton-Magaña, 2019).

Among natural colorless to faint yellow colored diamonds on the D-to-Z scale, approximately 35% fluoresce when exposed to long-wave UV light (Moses et al., 1997). While a rainbow of fluorescence colors are possible, the overwhelmingly most common color is blue (97%) due to emission by the N3 (N_3V^0) defect, as shown in figures 1, 3, and 4 (Moses et al., 1997; Luo and Breeding, 2013). Green fluorescence is usually caused by the H4 (ZPL at 496.2 nm, $N_4V_2^0$) or H3 (ZPL at 503.2 nm, N_2V^0) defects, but it can occasionally arise from the nickel-nitrogen-related S2 and S3 defects (ZPLs at 489.2 and 496.7 nm, respectively) (Clark et al., 1956; Collins, 1982, 1992; Eaton-Magaña et al., 2007; Yelisseyev and Kanda, 2007; Luo and Breeding, 2013). An overlapping combination of unidentified broad emission bands in the ~500–700 nm range are responsible for yellow to orange fluorescence (e.g., figure 4), most clearly detected in diamonds with 480 nm band absorption and in color-changing "chameleon" diamonds, though notably the fluorescence is not directly caused by the 480 nm band defect (Hainschwang et al., 2005; Eaton-Magaña et al., 2007; Fritsch et al., 2007; Luo and Breeding, 2013; Byrne et al., 2018; Lai et al., 2024). Finally, orange to red fluorescence can be produced by $NV^{0/-}$ defects (ZPLs at 575 and 637 nm, respectively) (Davies and Hamer, 1976; Collins, 1992; Eaton-Magaña et al., 2007; Luo and Breeding, 2013). This list is not exhaustive, and Shigley and Breeding (2013) provided a convenient diamond defect reference chart showing representative fluorescence images under long-wave and deep-UV (DiamondView) excitations. For natural diamonds, the fluorescence response is generally stronger to long-wave compared to short-wave UV, though there are exceptions.

The scientific definition of phosphorescence is complex, linked to the luminescence lifetime and the types of transitions that produce it (Nasdala and Fritsch, 2024). In practical terms, it is typically considered the emission of light after excitation is turned off (i.e., an "afterglow"). As a general guide, any emission lasting longer than 100 ns following excitation can be classified as phosphorescence. Most of the famous natural diamond examples are boron-contain-

Figure 4. Representative long-wave, short-wave, and deep-UV excited fluorescence and phosphorescence responses for D-to-Z color natural and laboratory-grown diamonds. Diamond origin details: blue-fluorescing natural (A), yellow-fluorescing natural (B), untreated CVD-grown (C), HPHT-annealed CVD-grown (D), and HPHT-grown (E). White light, long- and short-wave fluorescence, and phosphorescence images by Towfiq Ahmed. Deep-UV fluorescence and phosphorescence images by Ulrika F.S. D'Haenens-Johansson.

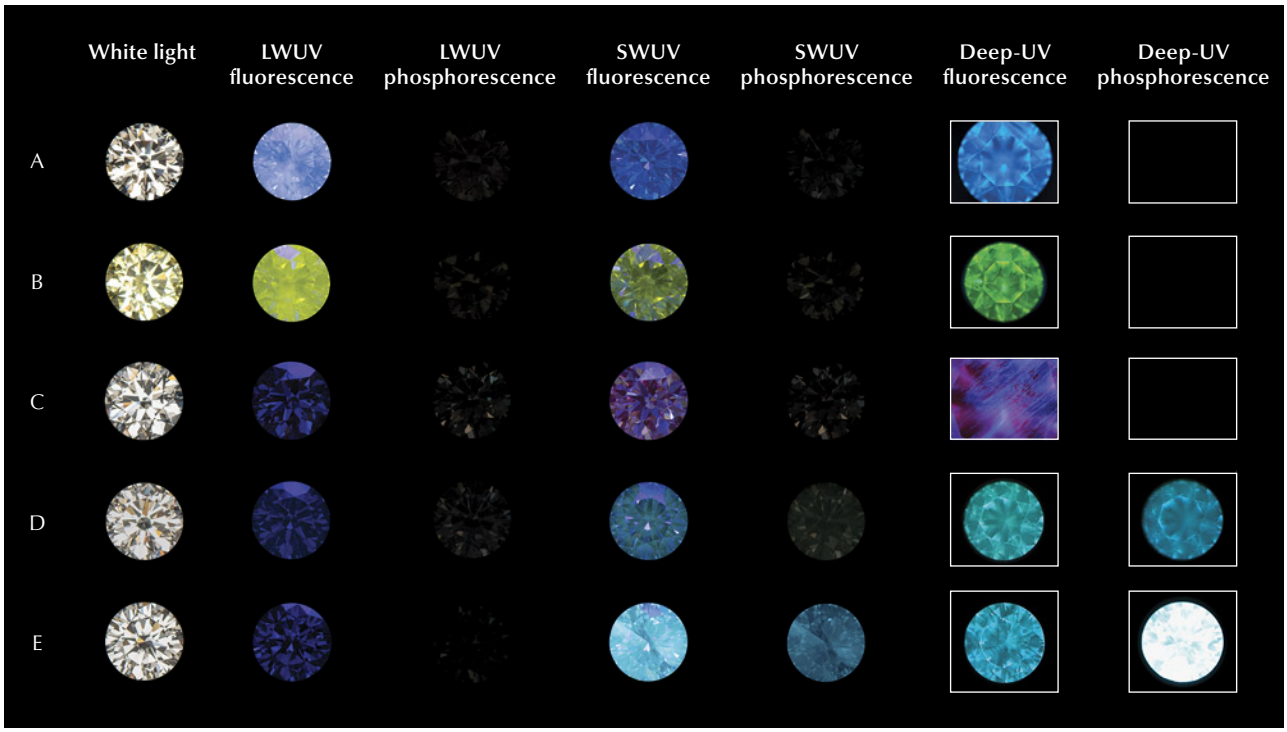

ing type IIb diamonds, which can show chalky blue to green, or rarely red or orangy red, phosphorescence following exposure to short-wave UV (Eaton-Magaña et al., 2008; Gaillou et al., 2010a). The phosphorescence can last from a few seconds to typically under a minute, though rare longer-lived natural examples exist (Shen and Eaton-Magaña, 2011). The phosphorescence is produced by two emission bands centered at 500 nm (blue-green) and 660 nm (red); the relative intensities and lifetimes determine the dominant phosphorescence color and its possible color evolution with time (Eaton-Magaña et al., 2008; Gaillou et al., 2010b; Eaton-Magaña and Lu, 2011). The mechanism used to explain the broad blue-green band is donor-acceptor pair recombination (DAP), where electrons bound to substitutional nitrogen defects (N_S^0, the donors) and holes bound to substitutional boron defects (B_S^0, the acceptors) are excited by the ultraviolet light, emitting phosphorescence as they recombine (Dean, 1965; Watanabe et al., 1997; Eaton-Magaña et al., 2008; Eaton-Magaña and Lu, 2011; Zhao et al., 2023). The detailed origin of the red band remains unexplained. Phosphorescence has also been reported for type I diamonds. Weak yellow and blue phosphorescence can be observed in strongly blue-fluorescing (N3) diamonds (Chandrasekharan, 1946a,b). Yellow phosphorescence following short-wave UV excitation, with a band centered at 550 nm, is considered a defining characteristic of color-changing "chameleon" diamonds (Hainschwang et al., 2005; Byrne et al., 2018; Lai et al., 2024).

The luminescence behavior of laboratory-grown diamonds produced by the high-pressure, high-temperature (HPHT) and chemical vapor deposition (CVD) methods has been studied extensively since their inception in the 1950s. For recent detailed reviews on the synthesis of diamond using these techniques, see Palyanov et al. (2015), Arnault et al. (2022), and D'Haenens-Johansson et al. (2022). These diamonds' fluorescence and phosphorescence properties, along with the distributions of the associated defects (discussed later in this article), have been exploited for diamond screening to separate natural from laboratory-grown diamonds, resulting in an assortment of device designs and approaches (Welbourn et al., 1996; Martineau et al., 2004; Hainschwang et al., 2013; Lan et al., 2016; Dupuy and Phillips, 2019; McGuinness et al., 2020; Tsai and D'Haenens-Johansson, 2021; Tsai et al., 2024).

Shigley et al. (2004a) and D'Haenens-Johansson et al. (2022) tabulated common fluorescence and phosphorescence characteristics for HPHT-grown diamonds produced with a range of bodycolors. Eaton-Magaña et al. (2017) analyzed several thousand HPHT-grown diamonds submitted to GIA from 2007 to 2016 and found that those showing fluorescence generally had a stronger reaction to short-wave UV than to long-wave UV, in contrast with most natural fluorescing diamonds. Since the majority of HPHT-grown diamond gemstones in the market today are colorless, including >90% of those submitted to GIA, it is appropriate to highlight their luminescence characteristics here (Eaton-Magaña et al., 2024). Among colorless and near-colorless HPHT-grown diamonds, the vast majority are inert to long-wave UV, with a yellow or orange emission if observed, while ~90% show yellow or yellow-green fluorescence to short-wave UV (Eaton-Magaña et al., 2017). Short-wave UV also induces an often strong and long-lived blue, yellow, or green-yellow phosphorescence that is associated with boron (Watanabe et al., 1997; Eaton-Magaña and Lu, 2011; Zhao et al., 2023). The range of phosphorescence colors observed are influenced by the intensities and lifetimes of a boron-related blue emission band centered at 500 nm and an orange or yellowish orange emission band whose center can range from 575 to 590 nm (Watanabe et al., 1997; Eaton-Magaña et al., 2008; Eaton-Magaña and Lu, 2011; D'Haenens-Johansson et al., 2015; Zhao et al., 2023). Figure 4 shows an example of the fluorescence and phosphorescence response of a colorless HPHT-grown diamond compared to that for natural and CVD-grown diamonds. It is, however, possible to reduce and even remove the phosphorescence through irradiation treatment, leaving screening instruments that rely on this feature vulnerable (Robinson, 2018; Dupuy and Phillips, 2019; Eaton-Magaña et al., 2024).

CVD-grown diamonds dominate the non-melee-sized laboratory-grown gem market; they currently account for ~80% of laboratory-grown diamond submissions to GIA (Eaton-Magaña et al., 2024). Of those, ~80% are graded as colorless. To achieve such high colors, CVD-grown diamonds are regularly subjected to HPHT or LPHT (low-pressure, high-temperature) annealing treatments, in which less desirable brown hues are reduced or removed (e.g., Martineau et al., 2004; Meng et al., 2008; Wang et al., 2012; Eaton-Magaña et al., 2021, 2024; D'Haenens-Johansson et al., 2022). These treatments modify the relative concentrations of defects in the material, resulting in changes to the fluorescence behavior. Early "as-grown" (untreated) CVD diamonds sometimes showed orange, orange-yellow, or yellow fluorescence

to both long- and short-wave UV (with a stronger response to the latter) from high concentrations of $NV^{0/-}$ defects (Martineau et al., 2004; Wang et al., 2007). Yet, as the colors and purity levels of as-grown products have improved, they are now nearly all inert under both long- and short-wave UV illumination (Eaton-Magaña et al., 2021); see, for instance, the sample shown in figure 4. Decolorizing annealing treatments reduce the relative concentration of NV centers while introducing green fluorescence from H3 (N_2V^0) defects or an unidentified defect with a ZPL at 499 nm and a complex vibronic band centered at ~550 nm; these treatments are most easily detected using short-wave UV (Martineau et al., 2004; Wang et al., 2012; Wassell et al., 2018; McGuinness et al., 2020). Weak blue-green phosphorescence associated with trace amounts of boron may also be introduced (Wang et al., 2012). The fluorescence and phosphorescence behavior for an HPHT-annealed colorless CVD diamond using long-wave, short-wave, and deep-UV illumination is shown in figure 4.

Spatial Distribution of Fluorescent and Phosphorescent Defects in Diamond: Analysis Using Deep-UV. Natural diamond can be pictured as growing outward from a nucleating core, supplied with carbon atoms from melts and fluids, deep in the earth's mantle at the high temperatures and pressures at which diamond—rather than its allotrope graphite—is stable. Sunagawa (1984) and Harris et al. (2022) presented comprehensive reviews of natural diamond *morphology*, or crystal shape. The ideal natural diamond rough morphology is octahedral: two square-based pyramids connected at the base with {111}-oriented faces.[1] The second most common morphology has well-developed, gently curved, and hummocky square faces that are approximately {100}-oriented. As they are not true {100} cubic faces, the preferred name for this morphology is *cuboid*. Diamonds can also experience mixed habit growth, though rarely observed, developing both octahedral and cuboid faces. By the time the diamond is recovered, the external morphology could be dramatically modified through geological processes, leading to rounded and irregular shapes. Furthermore, in the gem trade, the external surfaces are removed through polishing. Yet all is not lost: Conditions of natural diamond formation, their residence in the mantle, and subsequent transportation to the surface combine to leave an imprint.

Diamond growth progresses through a series of episodes, experiencing changes in the growth environment and the source fluid composition. Additionally, diamonds can potentially go through periods during which their surfaces are attacked by aggressive fluids, removing atoms and leading to crystal dissolution and resorption (Fedortchouk, 2019; Fedortchouk et al., 2019; Smit and Shirey, 2020; Harris et al., 2022). Diamonds may also be subjected to plastic deformation, introducing extended defects such as dislocations and glide planes (Evans and Wild, 1965; Willems et al., 2006; Laidlaw et al., 2020, 2021). As a result, the distributions, combinations, and relative concentrations of defects present in the crystal are heterogeneous, and every diamond has a unique and complex internal growth structure that reveals a fascinating history. One can think of these patterns as analogous to the growth rings present within a tree trunk, with variations caused by cyclical environmental changes as well as stressing conditions such as disease or insect infestations.

Since many diamond defects are luminescent, their distribution may be observed through fluorescence and phosphorescence, as well as electron-beam excited cathodoluminescence imaging (e.g., Welbourn et al., 1996; Harris et al., 2022). Although growth structure can occasionally be perceived through long-wave or short-wave UV illumination, the preferred excitation energy of incident photons is greater than diamond's band gap energy, here termed deep-UV, resulting in surface-specific emission from practically all diamonds (Welbourn et al., 1996). The characteristic fluorescence colors associated with specific luminescing defects described in the previous section remain unchanged, though the emission efficiency is generally improved using deep-UV illumination. Additionally, deep-UV illumination is able to excite blue to green "band A" emission (Dean, 1965; Ruan et al., 1992; Green et al., 2022). Recent high-resolution multi-technique studies by Laidlaw et al. (2020, 2021) have shown that band A originates from unidentified defects in the material adjacent to dislocations and grain boundaries, which themselves act as nonradiative recombination centers (i.e., they are dark). Importantly, the fundamental growth structure of a diamond, whether natural

[1]In crystallography, the Miller indices *h*, *k*, and *l* are used to mathematically define crystal planes and directions, enveloped by different forms of brackets and parentheses. Briefly, the notation is as follows: {*hkl*} represents planes that are symmetrically equivalent to a specific plane (*hkl*). [*hkl*] is a specific direction lying perpendicular to (*hkl*), whereas <*hkl*> is a group of directions that are equivalent to [*hkl*] by symmetry. For diamond, key crystallographic faces are the {111} octahedral, {100} cubic, and {110} dodecahedral faces.

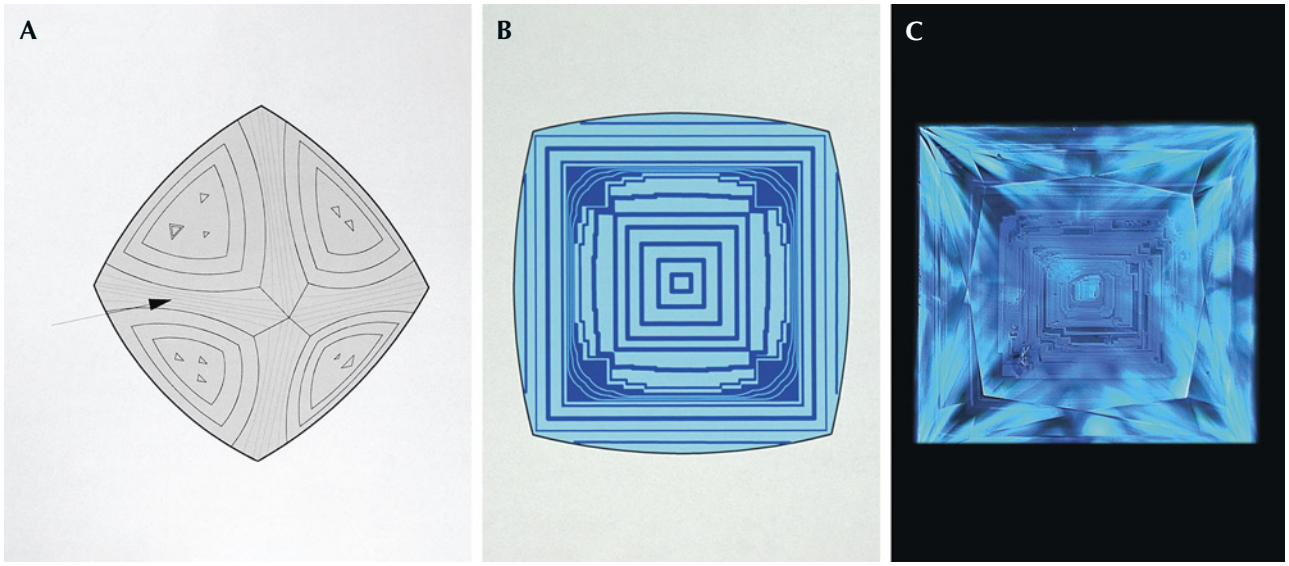

Figure 5. A: A representative illustration of a natural octahedral type Ia diamond crystal, showing rounded edges from resorption, as well as trigon etch pits. B: If the crystal was sliced along the central cubic {100} plane, the resulting distribution of fluorescent defects may show a series of concentric rectangles and hillocky rounded regions of cuboid growth. C: This 1.18 ct diamond displays an octahedral growth pattern when illuminated under deep-UV. Illustrations A and B are from Welbourn et al. (1996), and image C is from Chan (2009).

or laboratory-grown, cannot be changed by treatment, though the fluorescing colors can potentially be modified.

Internal growth patterns associated with natural octahedral diamond growth present themselves as a series of concentric squares or rectangles with varying luminescence, as shown in figure 5 (e.g., Welbourn et al., 1996; Harris et al., 2022). Depending on the crystallographic orientations of a polished diamond's facets and the viewing angle, the pattern may deviate from this ideal and appear truncated. Figure 6 shows a selection of natural diamond fluorescence patterns collected under deep-UV illumination. Cuboid growth introduces curved and hummocky growth horizons (figure 6A; Moore and Lang, 1972; Lang, 1974, 1979; Suzuki and Lang, 1976; Welbourn et al., 1989; Harris et al., 2022). Sometimes the internal growth patterns in natural diamond can be highly irregular or show multiple nucleation sites (figure 6B). Additionally, plastic deformation can introduce luminescent glide planes or dislocations (figure 6, C and D). Luminescence patterns in high-purity type IIa and boron-containing type IIb diamonds are typically dominated by polygonized dislocation networks (e.g., Hanley et al., 1977; De Corte et al., 2006; Smith et al., 2016, 2017; Smith, 2023), often emitting blue band A emission (figure 6E). High levels of natural irradiation can create structural damage to the diamond lattice, quenching luminescence, resulting in localized dark regions in fluorescence images, as shown in figure 6F (Schulze and Nasdala, 2016; Breeding et al., 2018; Smit et al., 2018; Breeding and Eaton-Magaña, 2019). Diamonds that phosphoresce under conventional UV excitation wavelengths, such as type IIb diamonds (e.g., figure 7), will also phosphoresce under deep-UV (e.g., Gaillou et al., 2010a; Eaton-Magaña and Lu, 2011; Eaton-Magaña et al., 2018). The response is typically more pronounced. With practice, these patterns can be recognized as natural, though complementary data is occasionally necessary for conclusive identification. Notably, treatments may or may not create changes in the fluorescence or phosphorescence colors, depending on the starting material and the treatment recipe (e.g., Hainschwang et al., 2008, 2009; Nasdala et al., 2013; Eaton-Magaña and Ardon, 2016; Wang et al., 2018; Breeding and Eaton-Magaña, 2019; Eaton-Magaña, 2020). Due to this variability, discussion is beyond the scope of this article.

The growth morphology of HPHT-grown diamonds is typically cuboctahedral, with well-developed cube {100} and octahedral {111} faces, with minor dodecahedral {110} and trapezohedral {113} faces (illustrated in figure 8), the balance of which can be affected by the growth temperatures (Strong and Chrenko, 1971; Kanda et al., 1980, 1989; Sunagawa, 1984, 1995; Satoh et al., 1990; Burns et al., 1999; Sumiya et al., 2002; D'Haenens-Johansson et

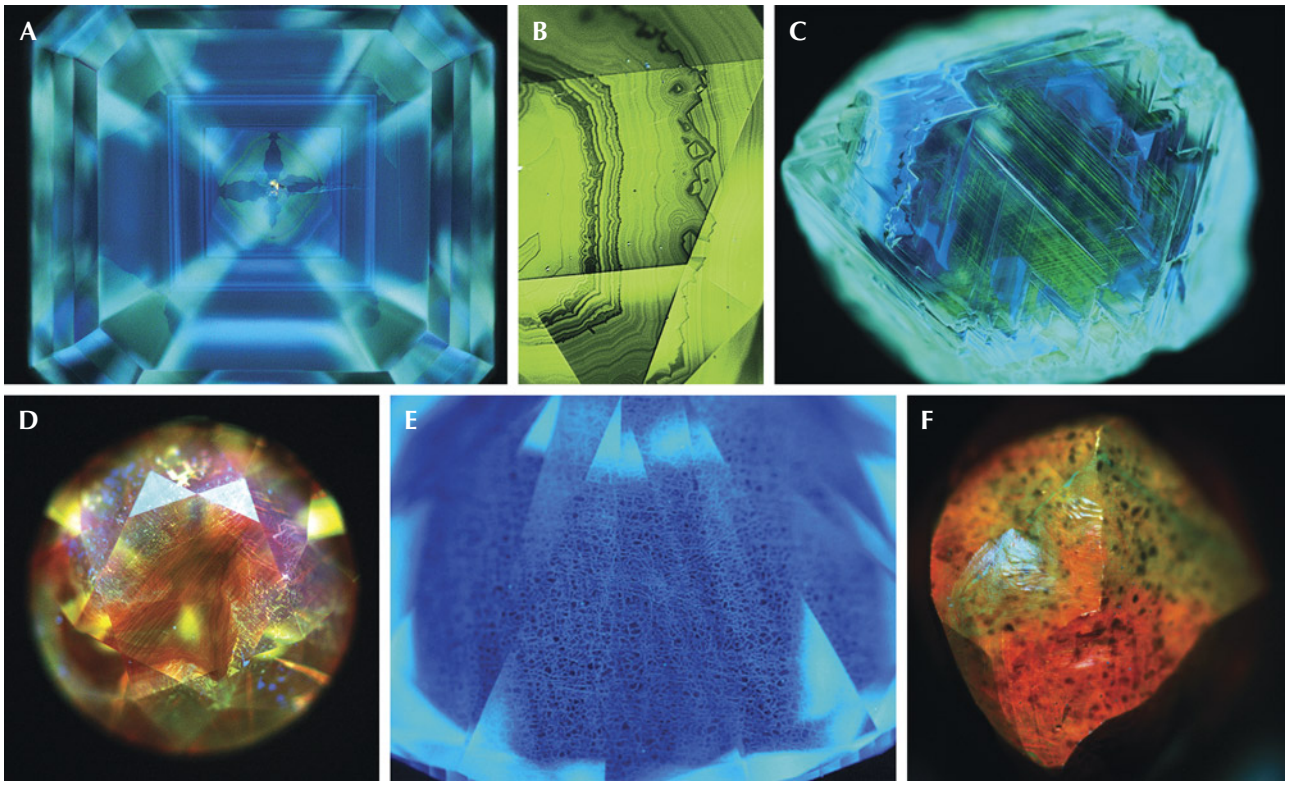

Figure 6. This selection of deep-UV fluorescence images of natural diamonds highlights the wide range of potential emission patterns and colors that can be observed, evidence of diamond's unique growth and residence history. E: Most natural type II diamonds show blue fluorescence with mosaic-like polygonized dislocation patterns, differing from characteristic type II CVD- or HPHT-grown diamond patterns (compare with figures 8–10). Images by Garrett Koneval (A), Najmeh Anjomani (B), Wuyi Wang (C), Christopher Vendrell (D), Ulrika F.S. D'Haenens-Johansson (E), and Sandeep Kabariya (F).

al., 2022). The uptake of impurities is strongly sector-dependent and sensitive to growth rates and temperatures (Strong and Chrenko, 1971; Burns et al., 1990, 1999; Satoh et al., 1990; Kiflawi et al., 2002). Boron concentrations are typically highest in {111} growth sectors, followed by {110} sectors; nitrogen concentrations follow a different order: {111} > {100} > {113} > {110} (Burns et al., 1990). The incorporation of nickel- and cobalt-related defects is also sector-dependent (Collins et al., 1990b; Lawson et al., 1996).

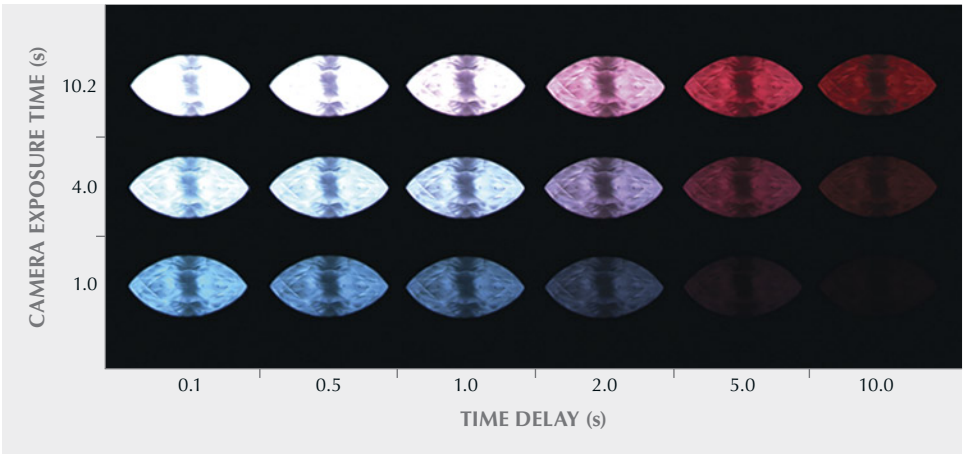

Figure 7. Following deep-UV illumination, the overall phosphorescence of natural type IIb diamonds may appear blue, gray, violet, or red due to emission bands centered at about 500 nm and/or 660 nm. From Moe and Johnson (2007).

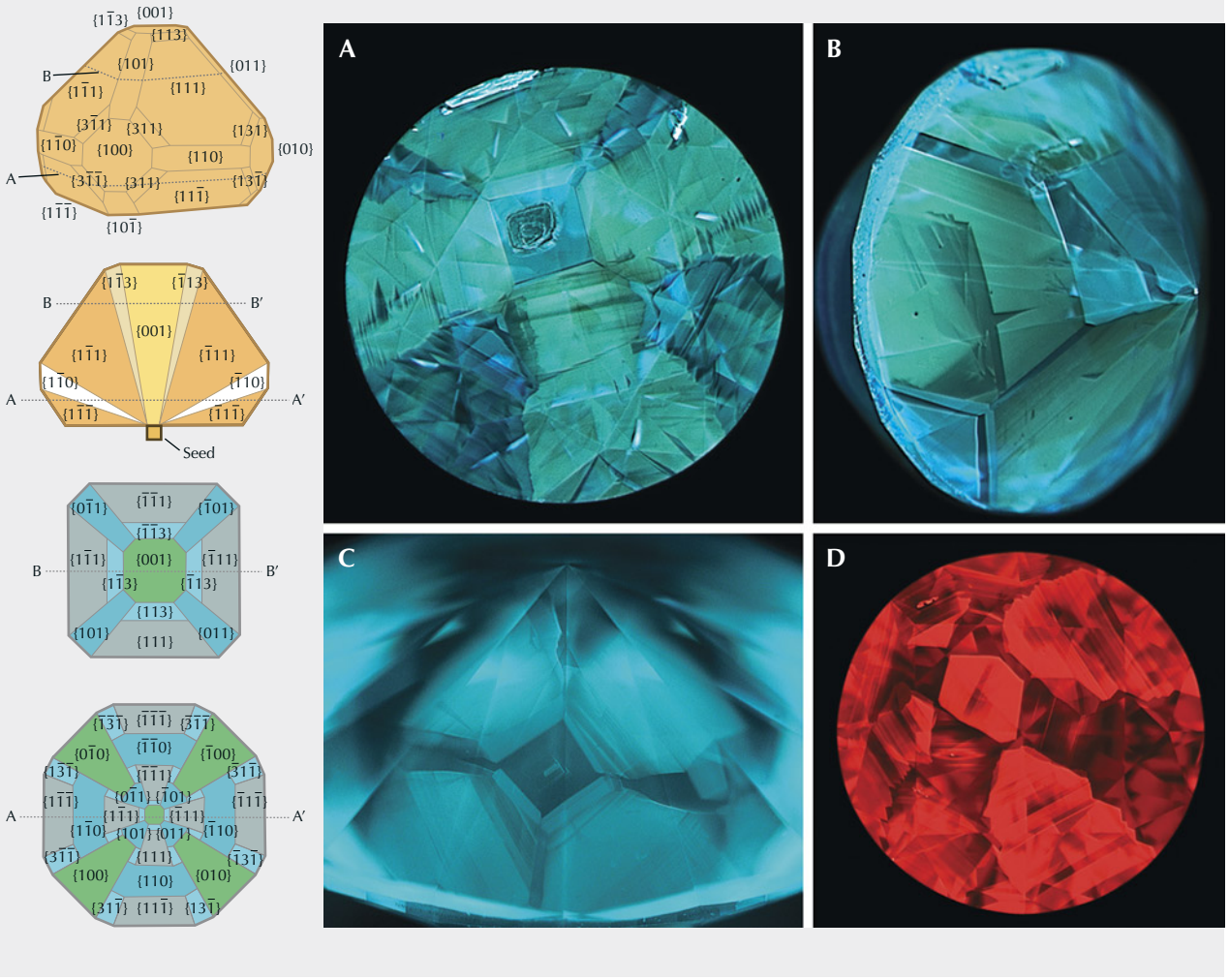

Figure 8. HPHT growth of diamonds typically results in crystals with a cuboctahedral morphology (top illustration), showing dominant octahedral {111} and cube {100} growth faces and minor dodecahedral {110} and trapezohedral {113} faces. The distribution of defects is highly heterogeneous, incorporating preferentially in certain growth sectors, shown as changing colors in the illustrations. The resulting characteristic sharp geometric growth patterns are apparent in deep-UV fluorescence images (A–D, where A and B are of the same sample), showing a range of fluorescence colors depending on growth chemistry and treatments. Colorless and near-colorless HPHT-grown diamonds, like this 4.07 ct E-color oval brilliant (C), typically show green-to-blue fluorescence followed by strong, long-lived phosphorescence. Illustrations from Welbourn et al. (1996).

In fancy-color HPHT-grown diamonds, the cuboctahedral distribution of defects may be noticeable under visible light, short-wave, and/or long-wave UV (e.g., Shigley et al., 2004a,b). Using deep-UV, the characteristic cuboctahedral growth patterns are enhanced (figure 8); this feature was largely the driving force for the development of the DiamondView instrument for diamond identification (Welbourn et al., 1996). The fluorescence colors depend on the concentration of defects, as summarized by Eaton-Magaña et al. (2017) and D'Haenens-Johansson et al. (2022). Colorless type II specimens fluoresce blue-green to green-blue, followed by remarkably long-lived green-blue (500 nm band) and/or yellow-orange (575 nm) phosphorescence, as shown in figure 8 (Watanabe et al., 1997; Eaton-Magaña et al., 2008, 2017; Eaton-Magaña and Lu, 2011; D'Haenens-Johansson et al., 2014, 2015; Zhao et al., 2023). The combination of the characteristic growth zonation, fluorescence color, and phosphorescence is recognizably different from what is observed for similarly colored natural and CVD-grown diamonds, making this a powerful tech-

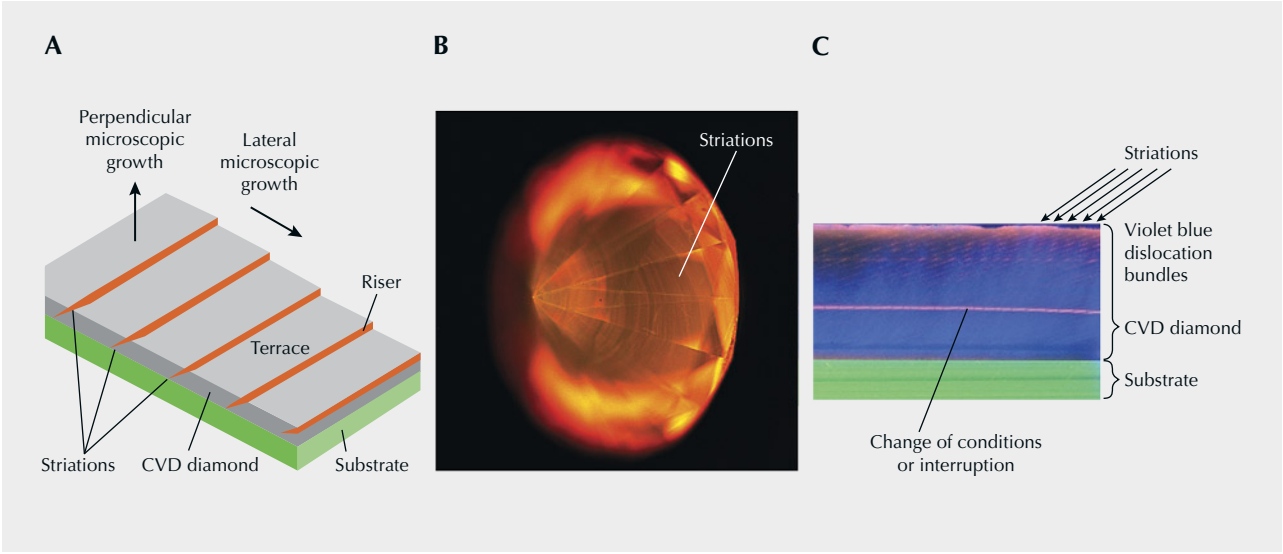

Figure 9. A: During the CVD growth process, diamond is deposited on a sacrificial diamond substrate as a series of flowing steps. Differences in defect incorporation between the risers and terraces form a pattern of tightly spaced striations. B: This 0.53 ct Fancy brownish pink untreated CVD-grown diamond shows a classic striation pattern, fluorescing orange from NV^0 defects under deep-UV illumination. C: Interruptions or changes in growth conditions can form either sharp or gradual interfaces that lie parallel to the main growth plane. Images A and C adapted from Martineau et al. (2004, 2009).

nique to differentiate between HPHT-grown and other diamond materials.

The CVD growth method is based on careful control of the gas-phase chemistry of a carbon-containing plasma that has been activated by a source of energy (typically microwaves), leading to diamond deposition on diamond seeds that act as the template for crystal growth. High-quality CVD diamond deposition usually occurs on (001)-oriented diamond seeds (also referred to as substrates), following what is known as "step-flow growth," with microscopic riser and terrace segments oriented along [001] and [101] directions, respectively (Martineau et al., 2004; 2009). The ensuing idealized layer-by-layer deposition produces a crystal with a cubic growth morphology. The different impurity uptake in the risers and terraces results in a heterogeneous incorporation of defects, creating a characteristic fluorescence pattern of tightly spaced striations that can be observed by deep-UV illumination (figure 9) (Martineau et al., 2004, 2009). Furthermore, any modifications to the growing conditions, whether unintentional or caused by planned interruptions, result in changes to the defect content in a plane parallel to the substrate, creating a layered appearance that depends on the viewing angle. This is a feature often observed in the deep-UV fluorescence images for large CVD-grown diamonds, presenting clear evidence they are produced through multiple-stage growth (e.g., Dieck et al., 2015; Law and Wang, 2016; Tam and Poon, 2023; Eaton-Magaña et al., 2024). Blue-fluorescing threading dislocations and bundles can also be observed, oriented in a direction approximately parallel to the main macroscopic growth direction, with deviations caused by the step-flow growth (Martineau et al., 2004, 2009). Notably, these dislocations may have a recognizably linear appearance when viewed along directions that transect the growth planes but can look patchy and nearly polygonized when the viewing angle is parallel to the main growth direction (Martineau et al., 2004, 2009; Dieck et al., 2015).

The fluorescence colors can span the entire visible spectrum, even for samples that are colorless. As-grown CVD diamonds generally show red, orange, or pink fluorescence colors from NV^0 defects, whereas the fluorescence colors of these nitrogen-containing CVD diamonds progress from yellow to green to turquoise with higher annealing temperatures (Martineau et al., 2004; Wang et al., 2012; Eaton-Magaña and Shigley, 2016; Wassell et al., 2018). Many annealed CVD diamonds also show green-blue phosphorescence (e.g., Wang et al., 2012). Eaton-Magaña and Myagkaya (2024) recently compared changes to the deep-UV images for a CVD-grown diamond that was

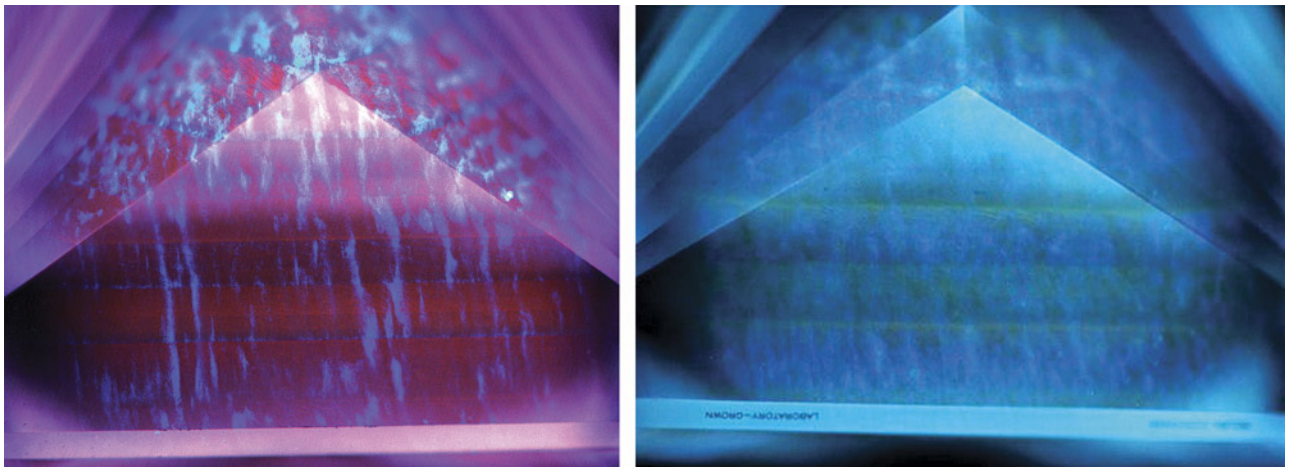

Figure 10. This CVD-grown diamond was examined before and after HPHT annealing treatments. Deep-UV fluorescence imaging highlights the changes in defect concentrations. Left: Untreated, it showed red emission from NV^0 defects. Right: After treatment, the fluorescence was dominated by shades of blues and greens from band A associated with dislocations and H3 (N_2V^0) defects, respectively. Notably, the layered pattern indicative of multi-stage CVD growth, as well as the violet blue–fluorescing dislocations, remain after treatment. The square modified brilliant sample was repolished, changing the weight from 16.41 ct to 15.73 ct. From Eaton-Magaña and Myagkaya (2024).

submitted to GIA before and after HPHT annealing (figure 10). The deep-UV fluorescence images illustrate luminescent defect concentration changes, highlighting that the sample's intrinsic growth pattern, characteristic of multi-stage CVD growth, was unaffected. CVD-grown diamonds that have been treated to produce blue, pink, or yellow bodycolors display similar characteristic patterns, but with different fluorescent colors depending on the defect content of the starting material and the treatment sequence (e.g., Wang et al., 2010; Moe et al., 2015; Eaton-Magaña and Shigley, 2016; Johnson et al., 2023).

Deep-UV imaging has also proven to be an invaluable tool in detecting rare CVD diamonds that are grown on natural diamonds, creating a "hybrid" natural/laboratory-grown diamond product (Fritsch and Phelps, 1993; Moe et al., 2017; Tang et al., 2018; Ardon and McElhenny, 2019). These examples were apparently produced to increase the sample weight or to create a potentially more valuable color, such as the blue hues introduced by type IIb CVD overgrowth layers. When exposed to deep-UV, the hybrid diamonds studied thus far have shown distinctive fluorescence patterns. The natural regions fluoresce blue due to N3 defects, while the CVD layers fluoresce red due to high NV^0 concentrations or, for cases of type IIb diamond deposition, fluoresce green-blue with similarly colored phosphorescence.

FLUORESCENCE AND PHOSPHORESCENCE BEHAVIOR OF OTHER GEMSTONES

Corundum. Lecoq de Boisbaudran (1887) demonstrated that pure alumina (i.e., corundum) was not luminescent but did show a red luminescence after doping with a small amount of chromium. This observation was later confirmed by several other researchers, including Nichols and Howes (1929). The red Cr^{3+} luminescence seen in ruby (e.g., figure 1) has been the subject of extensive research in the scientific and gemological literature (Ponahlo, 2000; Fritsch and Waychunas, 1994; Gaft and Panczer, 2013; Gaft et al., 2015). Ruby lasers, for instance, are based on the emission of chromium at 692.9 and 694.3 nm. Although this luminescence is commonly referred to as "fluorescence" in gemology and elsewhere, the excitation pathway for this feature means it should technically be classified as phosphorescence (Nasdala and Fritsch, 2024).

Fluorescence can be a useful tool for separating natural from synthetic rubies and identifying heat treatment in some rubies and sapphires (Hainschwang et al., 2013, 2024; Hughes et al., 2017; Mauthner, 2020). For instance, synthetic rubies are usually more strongly fluorescent than many natural rubies, as they generally lack iron. Synthetic rubies typically have strong red chromium-related fluorescence in long-wave UV and moderate to strong red

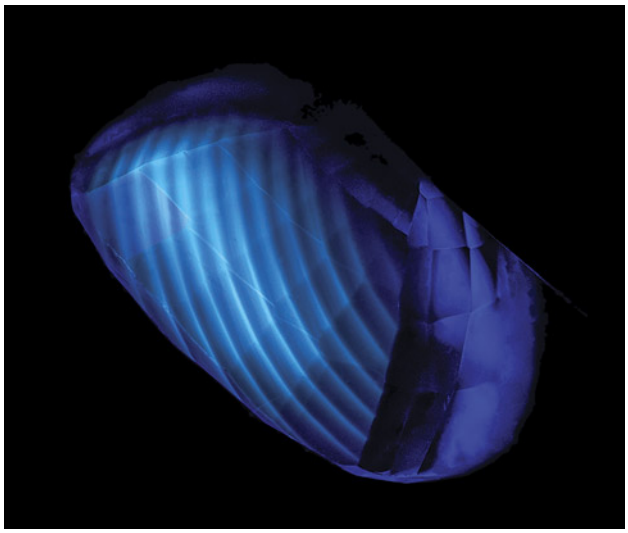

Figure 11. The curved banding in this flame-fusion synthetic blue sapphire is revealed by deep-UV illumination. From Hughes (2019); field of view ~10.4 mm.

fluorescence in short-wave UV. However, low-iron rubies from marble deposits such as Myanmar can show similar fluorescence intensities. Therefore, this test may support a natural versus synthetic determination, but it is insufficient on its own to fully separate these materials. Short-wave and deep-UV excitation can also provide insights into the growth structure of corundum. For example, they can enhance characteristic curved banding in flame-fusion synthetic sapphire, as shown in figure 11, which differs markedly from the angular growth patterns in natural stones (Hughes et al., 2017; Hughes, 2019; Zandi, 2021; Sohrabi and Anjomani, 2022; Hainschwang et al., 2024).

Fluorescence observations may also be helpful for identifying heat treatment. Many heat-treated low-iron sapphires and rubies show a chalky blue fluorescence under short-wave UV (figure 12) (Hughes and Emmett, 2005; Hughes et al., 2017; Hughes and Perkins, 2019; Hughes and Vertriest, 2022; Hainschwang et al., 2024). However, careful observation is needed, as red Cr^{3+} fluorescence can mask the chalky fluorescence (Mauthner, 2020). Notably, synthetic ruby and sapphire will often display this chalky fluorescence as well, although it can be masked by red fluorescence in some synthetic rubies. This bluish fluorescence often occurs in the wavelength range of 410–420 nm and is ascribed to the $O^{2-} \rightarrow Ti^{4+}$ charge-transfer transition (Evans, 1994; Wong et al., 1995a,b; Tsai et al., 2024). When heated, exsolved rutile (TiO_2) in corundum undergoes dissolution, creating Ti^{4+} ions and Ti-Al vacancies. The chalky bluish fluorescence coincides with rutile-containing zones but can be quenched by high iron concentrations (Hughes et al., 2017; Hughes and Perkins, 2019). This chalky reaction in heated corundum is almost never detected in natural corundum and was first documented by Crowningshield (1966, 1970). However, an inert reaction does not confirm that the stone is unheated, as the fluorescence bands can be destroyed at annealing temperatures above ~1500°C. The chalky reaction can be intensified if observed under deep-UV illumination

Figure 12. Left: A ruby sample tested by Hughes and Vertriest (2022) showed a strong red fluorescence in short-wave UV before heat treatment. Its appearance remained unchanged after heating to 600°, 750°, 900°, and 1100°C. Right: Zoned chalky fluorescence appeared following heating to 1500°C. From Hughes and Vertriest (2022).

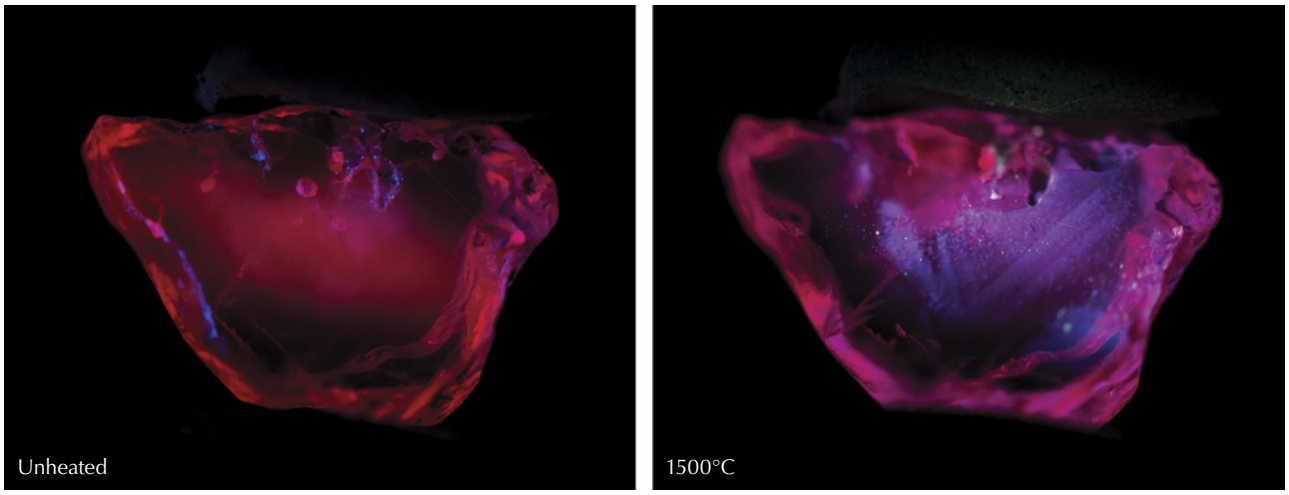

compared to short-wave UV, and it is possible that it can reveal lower-temperature annealing treatments (Hughes and Perkins, 2019).

Colored Stone Fracture Filling and Coatings. Although it is used far less commonly for colored stones than for diamonds, deep-UV fluorescence has proven useful in revealing different types of fracture-filling materials and potentially in estimating the degree of clarity enhancement. For example, surface-reaching glass filler in clarity-enhanced rubies can fluoresce blue, in sharp contrast to the red Cr^{3+} emission from the host (Lai, 2018a). Filtering the emission signal using a blue band-pass filter reduces the intensity of the red background emission, facilitating detection of the filler's fluorescence. Similar results were found for emeralds that had been clarity enhanced with epoxy resin fillers or oils, with the fluorescence color providing clues to the filler's identity (Notari et al., 2002; Hainschwang et al., 2013; Droux and Fritsch, 2015; Lai, 2018b; Gaievskyi, 2022). Fluorescence from fillers may also be observed in emeralds using long-wave UV illumination due to the mineral's often weak to undetectable Cr^{3+} fluorescence, as shown in figure 13 (e.g., Tsai, 2021). Untreated jadeite is typically inert, but fluorescence testing can provide evidence of coating, dyeing, and impregnation (Lu, 2012; Zhang and Shen, 2023). Waxes and epoxy resins used to impregnate jadeite may fluoresce blue under long-wave UV illumination (Lai, 2016, 2018c); the response can be more pronounced using deep-UV excitation, with epoxy resin forming a complex weblike fluorescence pattern. Coated jadeite may also be identified by differences in fluorescence color and intensity between the coating and any exposed jadeite (Zhang et al., 2013).

Figure 13. The epoxy filling of this clarity-enhanced emerald fluoresces blue under 365 nm illumination. From Tsai (2021).

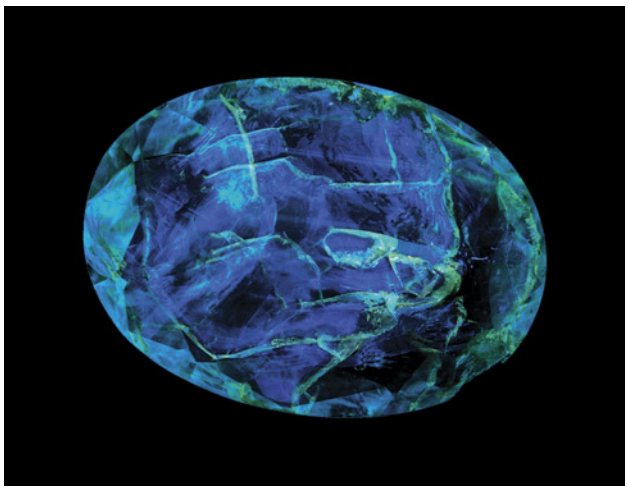

Pearls. Pearls are organic gemstones produced by various saltwater and freshwater mollusk species, with radial layers consisting of calcium carbonate crystals held together by a mixture of organic matrix that is often referred to as conchiolin. Most are nacreous, where the calcium carbonate is in the form of aragonite platelets, while the less common non-nacreous pearls have a different aragonite structure or, in some cases, are composed of calcite instead of aragonite (figure 14). Pearls can be natural or cultured and may undergo a range of treatments to improve their appearance, including dyeing, bleaching, optical brightening, irradiation, or *maeshori* luster enhancement.

UV fluorescence analysis of pearls is neither straightforward nor conclusive (Fritsch and Waychunas, 1994). Pearls may fluoresce under long-wave UV, with a rainbow of colors and intensities that are influenced by several factors, including treatments and the intensity of bodycolor (Elen, 2001; Kiefert et al., 2004; Wang et al., 2006; Sturman et al., 2014, 2019; Zhou et al., 2012, 2016, 2020, 2021; Tsai and Zhou, 2021). Generally, darker or more saturated colors fluoresce more weakly. Untreated white to cream-colored pearls often show blue or greenish blue fluorescence, yet processed pearls such as akoya and cultured freshwater pearls can fluoresce a strong bluish white (Zhou et al., 2020). Strong bluish fluorescence to long-wave UV also raises the suspicion that a pearl has been subjected to optical brightening, where an optical brightening agent (OBA) has been added to counteract less valuable yellow hues by intensifying or introducing blue fluorescence (~430 nm) (Zhou et al., 2020, 2021). Fluorescence from OBAs is not as efficiently excited by short-wave UV. Yet short-wave UV can induce fluorescence from the naturally occurring amino acid tryptophan (Trp or W) that is present in pearl nacre, and its intensity may be reduced by color treatments and processing (Tsai and Zhou, 2021; Tsai et al., 2024). As its emission is centered at ~340 nm, with a higher wavelength tail ending at ~450 nm, its fluorescence is only weakly blue and difficult to detect visually.

The range of fluorescence behaviors observed for pearls and their overlapping emissions makes visual analysis challenging. Fluorescence spectroscopy using

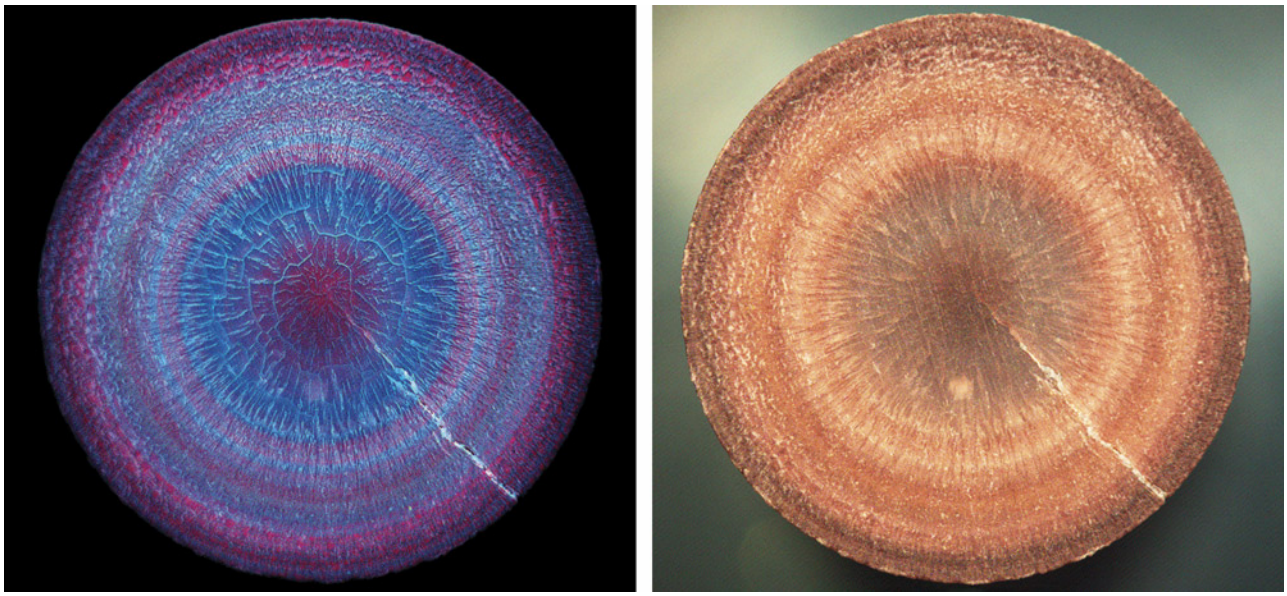

Figure 14. Left: Deep-UV fluorescence of this 0.51 ct non-nacreous natural pearl cross section (~6.57 mm diameter) reveals its concentric calcite growth structure, held together by inert conchiolin. Right: The fluorescence colors are associated with variations in the natural pigments, seen under white light. The original pearl weighed 2.18 ct and was reportedly from a Pinctada radiata *mollusk from the waters off Kuwait. Images by Ravenya Atchalak.*

different excitation sources shows promise for gemological applications, as it allows separation and identification of the fluorescing components, though a comprehensive assessment still requires multi-technique analysis (Miyoshi et al., 1987; Miyoshi, 1992; Iwahashi and Akamatsu, 1994; Ju et al., 2011; Shi et al., 2018; Zhou et al., 2016, 2020, 2021; Tsai and Zhou, 2021; Tsai et al., 2024).

CONCLUSIONS

Luminescence analysis can elucidate much about a gemstone's history and whether it is natural, laboratory-grown, or treated. The luminescence arises from impurity and defect structures in the crystal lattice and can be detected even at concentrations as low as a few parts per billion. Imaging methods based on photoluminescence, comprising fluorescence and phosphorescence, are particularly powerful analytical tools because they reveal characteristic luminescent defect distributions using simple ultraviolet light sources. This has made it a valuable technique for gemologists and scientists alike.

For example, the distribution of luminescent defects in gem diamond can help distinguish between natural and laboratory-grown crystals. It can also provide clues into any post-growth processes the diamond may have undergone, either naturally or through artificial treatment. Phosphorescence is rare enough in natural diamonds that any phosphorescent diamond should be fully analyzed to determine its method of formation. Although most commonly used for diamond research, fluorescence and phosphorescence investigations of other gemstones are also plentiful.

Natural and synthetic growth structures for other materials, including corundum and pearls, have also been revealed under UV illumination. Furthermore, any treatments applied to these gems may alter their fluorescence. Coatings, dyes, and fracture filling of corundum, emerald, and jade can be highlighted using fluorescence imaging, as these foreign substances have fluorescence responses that differ from the host gem. A deeper understanding of fluorescing materials, and their corresponding spectra, has resulted in key advances in instrumentation, optimizing illumination wavelengths to selectively enhance certain features. Consequently, luminescence imaging has become an indispensable tool for material analysis, one that is routinely used in gemological laboratories. The largely straightforward interpretation of gemstone fluorescence and phosphorescence behaviors, coupled with their distinctive patterns, makes these techniques valuable for those in the trade as well. The low cost and ease of operating fluorescence and phosphorescence imaging systems compared to alternative luminescence techniques such as cathodoluminescence further increase their accessibility and appeal.

ABOUT THE AUTHORS
Dr. Ulrika D'Haenens-Johansson is senior manager of diamond research, Dr. W. Henry Towbin is a postdoctoral research associate, and Elina Myagkaya is a research associate, at GIA in New York. Dr. Sally Eaton-Magaña is senior manager of diamond identification at GIA in Carlsbad, California.

ACKNOWLEDGMENTS
Dr. Towbin is supported by the Richard T. Liddicoat Postdoctoral Research Associate Fellowship at GIA. We would like to thank Christopher M. Welbourn, Simon C. Lawson, James E. Butler, and Aaron C. Palke for their manuscript feedback, as well as Chunhui Zhou and Tsung-Han Tsai for their illuminating comments on pearl luminescence. Rachelle Turnier is acknowledged for identifying some relevant references on colored stone fluorescence. We are also grateful to Christopher M. Breeding for providing the N3 fluorescence data presented in figure 3. Finally, we are thankful to the GIA identification and analytics teams who have collected countless fluorescence and phosphorescence images over the years, providing the backbone for this article.

REFERENCES

Anderson B.W. (1943) Absorption and luminescence of diamonds. *The Gemmologist*, Vol. 12, No. 138, pp. 21–22; No. 139, pp. 25–27; No. 141, pp. 33–35.

Ardon T., McElhenny G. (2019) Lab Notes: CVD layer grown on natural diamond. *G&G*, Vol. 55, No. 1, pp. 97–99.

Arnault J.-C., Saada S., Ralchenko V. (2022) Chemical vapor deposition single-crystal diamond: A review. *Physica Status Solidi Rapid Research Letters*, Vol. 16, No. 1, article no. 2100354, http://dx.doi.org/10.1002/pssr.202100354

Barjon J. (2017) Luminescence spectroscopy of bound excitons in diamond. *physica status solidi (a)*, Vol. 214, No. 11, article no. 1700402, http://dx.doi.org/10.1002/pssa.201700402

Boyle R. (1664) *Experiments and Considerations Touching Colours: First Occasionally Written, Among Some Other Essays to a Friend, and Now Suffer'd to Come Abroad as the Beginning of an Experimental History of Colours*. Herringman, London.

Breeding C.M., Eaton-Magaña S. (2019) Fluorescence of natural and synthetic gem diamond: Mechanism and applications. In R.A. Meyers, Ed., *Encyclopedia of Analytical Chemistry*, Wiley & Sons, pp. 1–24, https://doi.org/10.1002/9780470027318.a9670

Breeding C.M., Eaton-Magaña S., Shigley J.E. (2018) Natural-color green diamonds: A beautiful conundrum. *G&G*, Vol. 54, No. 1, pp. 2–27, http://dx.doi.org/10.5741/GEMS.54.1.2

Burns R.C., Cvetkovic V., Dodge C.N., Evans D.J.F., Rooney M.L.T., Spear P.M., Welbourn C.M. (1990) Growth-sector dependence of optical features in large synthetic diamonds. *Journal of Crystal Growth*, Vol. 104, No. 2, pp. 257–279, http://dx.doi.org/10.1016/0022-0248(90)90126-6

Burns R.C., Hansen J.O., Spits R.A., Sibanda M., Welbourn C.M., Welch D.L. (1999) Growth of high purity large synthetic diamond crystals. *Diamond and Related Materials*, Vol. 8, No. 8-9, pp. 1433–1437, http://dx.doi.org/10.1016/S0925-9635(99)00042-4

Byrne K.S., Butler J.E., Wang W., Post J.E. (2018) Chameleon diamonds: Thermal processes governing luminescence and a model for the color change. *Diamond and Related Materials*, Vol. 81, pp. 45–53, http://dx.doi.org/10.1016/j.diamond.2017.10.014

Chan S. (2009) Lab Notes: Unusual trigon-shaped clouds indicate two diamonds cut from the same piece of rough. *G&G*, Vol. 45, No. 4, p. 291–292.

Chandrasekharan V. (1946a) The thermoluminescence of diamond. *Proceedings of the Indian Academy of Sciences – Section A*, Vol. 24, No. 1, article no. 187, http://dx.doi.org/10.1007/BF03170755

——— (1946b) The phosphorescence of diamond. *Proceedings of the Indian Academy of Sciences – Section A*, Vol. 24, No. 1, article no. 193, http://dx.doi.org/10.1007/BF03170756

Clark C.D., Ditchburn R.W., Dyer H.B. (1956) The absorption spectra of natural and irradiated diamonds. *Proceedings of the Royal Society of London, Series A*, Vol. 234, No. 1198, pp. 365–381, http://dx.doi.org/10.1098/rspa.1956.0040

Clark C.D., Dean P.J., Harris P.V. (1964) Intrinsic edge absorption in diamond. *Proceedings of the Royal Society of London, Series A*, Vol. 277, No. 1370, pp. 312–329, http://dx.doi.org/10.1098/rspa.1964.0025

Collins A.T. (1982) Colour centres in diamond. *Journal of Gemmology*, Vol. 18, No. 1, pp. 37–75.

——— (1992) The characterisation of point defects in diamond by luminescence spectroscopy. *Diamond and Related Materials*, Vol. 1, No. 5-6, pp. 457–469, http://dx.doi.org/10.1016/0925-9635(92)90146-F

——— (1993) Intrinsic and extrinsic absorption and luminescence in diamond. *Physica B: Condensed Matter*, Vol. 185, No. 1-4, pp. 284–296, http://dx.doi.org/10.1016/0921-4526(93)90250-A

Collins A.T., Lawson S.C., Davies G., Kanda H. (1990a) Indirect energy gap of ^{13}C diamond. *Physical Review Letters*, Vol. 65, No. 7, pp. 891–894, http://dx.doi.org/10.1103/PhysRevLett.65.891

Collins A.T., Kanda H., Burns R.C. (1990b) The segregation of nickel-related optical centres in the octahedral growth sectors of synthetic diamond. *Philosophical Magazine B*, Vol. 61, No. 5, pp. 797–810, http://dx.doi.org/10.1080/13642819008207562

Crossfield M.D., Davies G., Collins A.T., Lightowlers E.C. (1974) The role of defect interactions in reducing the decay time of H3 luminescence in diamond. *Journal of Physics C: Solid State Physics*, Vol. 7, No. 10, pp. 1909–1917, http://dx.doi.org/10.1088/0022-3719/7/10/018

Crowningshield R. (1966) Developments and Highlights at the Gem Trade Lab in New York: Unusual items encountered [sapphire with unusual fluorescence]. *G&G*, Vol. 12, No. 3, p. 73.

——— (1970) Developments and Highlights at GIA's Lab in New York: Unusual fluorescence. *G&G*, Vol. 13, No. 4, pp. 120–122.

Davies G., Crossfield M. (1973) Luminescence quenching and zero-phonon line broadening associated with defect interactions in diamond. *Journal of Physics C: Solid State Physics*, Vol. 6, No. 5, pp. L104–L108, http://dx.doi.org/10.1088/0022-3719/6/5/007

Davies G., Hamer M.F. (1976) Optical studies of the 1.945 eV vibronic band in diamond. *Proceedings of the Royal Society of London A*, Vol. 348, No. 1653, pp. 285–298, http://dx.doi.org/10.1098/rspa.1976.0039

Davies G., Welbourn C.M., Loubser J.H.N. (1978) Optical and electron paramagnetic effects in yellow type Ia diamonds. In P. Daniel, Ed., *Diamond Research*, Industrial Diamond Information Bureau, Ascot, UK, pp. 23–30.

Davies G., Thomaz M.F., Nazare M.H., Martin M.M., Shaw D. (1987) The radiative decay time of luminescence from the vacancy in diamond. *Journal of Physics C: Solid State Physics*, Vol. 20, No. 1, pp. L13–L17, http://dx.doi.org/10.1088/0022-3719/20/1/003

Dean P.J. (1965) Bound excitons and donor-acceptor pairs in natural and synthetic diamond. *Physical Review*, Vol. 139, No. 2A, article no. A588, http://dx.doi.org/10.1103/PhysRev.139.A588

De Corte K., Anthonis A., Van Royen J., Blanchaert M., Barjon J., Willems B. (2006) Overview of dislocation networks in natural type IIa diamonds. *G&G*, Vol. 42, No. 3, pp. 122–123.

De Ment J. (1949) *Handbook of Fluorescent Gems and Minerals – An Exposition and Catalog of the Fluorescent and Phosphorescent Gems and Minerals, Including the Use of Ultraviolet Light in the Earth Sciences*. Mineralogist Publishing Company, Portland, Oregon.

D'Haenens-Johansson U.F.S., Moe K.S., Johnson P., Wong S.Y., Lu R., Wang W. (2014) Near-colorless HPHT synthetic diamonds from AOTC Group. *G&G*, Vol. 50, No. 1, pp. 30–45, http://dx.doi.org/10.5741/GEMS.50.1.30

D'Haenens-Johansson U.F.S., Katrusha A., Moe K.S., Johnson P., Wang W. (2015) Large colorless HPHT-grown synthetic gem diamonds from New Diamond Technology. Russia. *G&G*, Vol. 51, No. 3, pp. 260–279, http://dx.doi.org/10.5741/GEMS.51.3.260

D'Haenens-Johansson U.F.S., Butler J.E., Katrusha A.N. (2022) Synthesis of diamonds and their identification. *Reviews in Mineralogy & Geochemistry*, Vol. 88, No. 1, pp. 689–753, http://dx.doi.org/10.2138/rmg.2022.88.13

Dieck C., Loudin L., D'Haenens-Johansson U.F.S. (2015) Lab Notes: Two large CVD-grown synthetic diamonds tested by GIA. *G&G*, Vol. 51, No. 4, pp. 437–439.

Droux A., Fritsch E. (2015) Gem News International: An unusual filled ruby. *G&G*, Vol. 51, No. 2, pp. 206–208.

Dupuy H., Phillips J.C. (2019) Selecting a diamond verification instrument based on the results of the Assure Program: An initial analysis. *Journal of Gemmology*, Vol. 36, No. 7, pp. 606–619.

Dyer H.B., Matthews I.G. (1958) The fluorescence of diamond. *Proceedings of the Royal Society of London A*, Vol. 243, No. 1234, pp. 320–335, http://dx.doi.org/10.1098/rspa.1958.0002

Eaton-Magaña S. (2020) Lab Notes: Irradiated blue diamond with interesting DiamondView image. *G&G*, Vol. 56, No. 2, p. 283.

Eaton-Magaña S., Ardon T. (2016) Temperature effects on luminescence centers in natural type IIb diamonds. *Diamond and Related Materials*, Vol. 69, pp. 86–95, http://dx.doi.org/10.1016/j.diamond.2016.07.002

Eaton-Magaña S., Lu R. (2011) Phosphorescence in type IIb diamonds. *Diamond and Related Materials*, Vol. 20, No. 7, pp. 983–989, http://dx.doi.org/10.1016/j.diamond.2011.05.007

Eaton-Magaña S., Myagkaya E. (2024) Lab Notes: Large CVD-grown diamond resubmitted after HPHT treatment. *G&G*, Vol. 60, No. 1, pp. 61–63.

Eaton-Magaña S., Shigley J.E. (2016) Observations on CVD-grown synthetic diamonds: A review. *G&G*, Vol. 52, No. 3, pp. 222–245, http://dx.doi.org/10.5741/GEMS.52.3.222

Eaton-Magaña S., Post J.E., Heaney P.J., Walters R.A., Breeding C.M., Butler J.E. (2007) Fluorescence spectra of colored diamonds using a rapid, mobile spectrometer. *G&G*, Vol. 43, No. 4, pp. 332–351, http://dx.doi.org/10.5741/GEMS.43.4.332

Eaton-Magaña S., Post J.E., Heaney P.J., Freitas J., Klein P., Walters R., Butler J.E. (2008) Using phosphorescence as a fingerprint for the Hope and other blue diamonds. *Geology*, Vol. 36, No. 1, pp. 83–86, http://dx.doi.org/10.1130/G24170A.1

Eaton-Magaña S., Shigley J.E., Breeding C.M. (2017) Observations on HPHT-grown synthetic diamonds: A review. *G&G*, Vol. 53, No. 3, pp. 262–284, http://dx.doi.org/10.5741/GEMS.53.3.262

Eaton-Magaña S., Breeding C.M., Shigley J.E. (2018) Natural-color blue, gray, and violet diamonds: Allure of the deep. *G&G*, Vol. 54, No. 2, pp. 112–131, http://dx.doi.org/10.5741/GEMS.54.2.112

Eaton-Magaña S., Ardon T., Breeding C.M. (2021) Laboratory-grown diamond: A gemological laboratory perspective. *Journal of Gems & Gemmology*, Vol. 23, No. 6, pp. 25–39.

Eaton-Magaña S., Hardman M.F., Odake S. (2024) Laboratory-grown diamonds: An update on identification and products evaluated at GIA. *G&G*, Vol. 60, No. 2, pp. 146–167, http://dx.doi.org/10.5741/GEMS.60.2.146

Elen S. (2001) Spectral reflectance and fluorescence characteristics of natural-color and heat-treated "golden" South Sea cultured pearls. *G&G*, Vol. 37, No. 2, pp. 114–123, http://dx.doi.org/10.5741/GEMS.37.2.114

Evans B.D. (1994) Ubiquitous blue luminescence from undoped synthetic sapphires. *Journal of Luminescence*, Vol. 60–61, pp. 620–626, http://dx.doi.org/10.1016/0022-2313(94)90233-X

Evans T., Wild R.K. (1965) Plastic bending of diamond plates. *Philosophical Magazine*, Vol. 12, No. 117, pp. 479–489, http://dx.doi.org/10.1080/14786436508218894

Fedortchouk Y. (2019) A new approach to understanding diamond surface features based on a review of experimental and natural diamond studies. *Earth Science Review*, Vol. 193, pp. 45–65, http://dx.doi.org/10.1016/j.earscirev.2019.02.013

Fedortchouk Y., Liebske, C., McCammon C. (2019) Diamond destruction and growth during mantle metasomatism: An experimental study of diamond resorption features. *Earth and Planetary Science Letters*, Vol. 506, pp. 493–506, http://dx.doi.org/10.1016/j.epsl.2018.11.025

Fritsch E., Phelps A.W. (1993) Type IIb diamond thin films deposited onto near-colorless natural gem diamonds. *Diamond and Related Materials*, Vol. 2, No. 2-4, pp. 70–74, http://dx.doi.org/10.1016/0925-9635(93)90033-X

Fritsch E., Massi L., Rossman G.R., Hainschwang T., Jobic S., Dessapt R. (2007) Thermochromic and photochromic behaviour of "chameleon" diamonds. *Diamond and Related Materials*, Vol. 16, No. 2, pp. 401-408, http://dx.doi.org/10.1016/j.diamond.2006.08.014

Fritsch E., Waychunas G.A. (1994) Gemstones. In M. Robbins, Ed., *Fluorescence: Gems and Minerals Under Ultraviolet Light*, Geoscience Press Inc., Phoenix.

Gaft M., Panczer G. (2013) Laser-induced time-resolved luminescence spectroscopy of minerals: A powerful tool for studying the nature of emission centres. *Mineralogy and Petrology*, Vol. 107, No. 3, pp. 363–372, http://dx.doi.org/10.1007/s00710-013-0293-3

Gaft M., Reisfeld R., Panczer G. (2015) *Modern Luminescence Spectroscopy of Minerals and Materials*, 2nd ed., Springer-Verlag, Berlin and Heidelberg.

Gaievskyi I. (2022) Gem News International: Unusual repair of a natural emerald. *G&G*, Vol. 58, No. 1, pp. 118–120.

Gaillou E., Wang W., Post J.E., King J.M., Butler J.E., Collins A.T., Moses T.M. (2010a) The Wittelsbach-Graff and Hope diamonds: Not cut from the same rough. *G&G*, Vol. 46, No. 2, pp. 80–88, http://dx.doi.org/10.5741/GEMS.46.2.80

Gaillou E., Post J.E., Bassim N.D., Zaitsev A.M., Rose T., Fries M.D., Stroud R.M., Steele A., Butler J.E. (2010b) Spectroscopic and microscopic characterizations of color lamellae in natural pink diamonds. *Diamond and Related Materials*, Vol. 19, No. 10, pp. 1207–1220, http://dx.doi.org/10.1016/j.diamond.2010.06.015

Green B.L., Breeze B.G., Newton M.E. (2017) Electron paramagnetic resonance and photochromism of N_3V^0 in diamond. *Journal of Physics: Condensed Matter*, Vol. 29, No. 22, article no. 225701, http://dx.doi.org/10.1088/1361-648X/aa6c89

Green B.L., Collins A.T., Breeding C.M. (2022) Diamond spectroscopy, defect centers, color, and treatments. *Reviews in Mineralogy and Geochemistry*, Vol. 88, No. 1, pp. 637–688, http://dx.doi.org/10.2138/rmg.2022.88.12

Hainschwang T., Simic D., Fritsch E., Deljanin B., Woodring S., DelRe N. (2005) A gemological study of a collection of chameleon diamonds. *G&G*, Vol. 41, No. 1, pp. 2–17, http://dx.doi.org/10.5741/GEMS.41.1.20

Hainschwang T., Notari F., Fritsch E., Massi L. Rondeau B., Breeding C.M., Vollstaedt H. (2008) HPHT treatment of CO_2 containing and CO_2-related brown diamonds. *Diamond and Related Materials*, Vol. 17, No. 3, pp. 340–351, http://dx.doi.org/10.1016/j.diamond.2008.01.022

Hainschwang T., Respinger A., Notari F., Hartmann H.J., Günthard C. (2009) A comparison of diamonds irradiated by high fluence neutrons or electrons, before and after annealing. *Diamond and Related Materials*, Vol. 18, No. 10, pp. 1223–1234,

http://dx.doi.org/10.1016/j.diamond.2009.04.011
Hainschwang T., Karampelas S., Fritsch E., Notari F. (2013) Luminescence spectroscopy and microscopy applied to study gem materials: A case study of C centre containing diamonds. *Mineralogy and Petrology*, Vol. 107, No. 3, pp. 393–413, http://dx.doi.org/10.1007/s00710-013-0273-7
Hainschwang T., Fritsch, E., Gaillou E., Shen A. (2024) Analysing the luminescence of gems. *Elements*, Vol. 20, No. 5, pp. 312–317, http://dx.doi.org/10.2138/gselements.20.5.312
Hanley P.L., Kiflawi I., Lang A.R. (1977) On topographically identifiable sources of cathodoluminescence in natural diamonds. *Philosophical Transactions of the Royal Society – Series A*, Vol. 284, No. 1324, pp. 329–368, http://dx.doi.org/10.1098/rsta.1977.0012
Harris J.W., Smit K.V., Fedortchouk Y., Morre M. (2022) Morphology of monocrystalline diamond and its inclusions. *Reviews in Mineralogy and Geochemistry*, Vol. 88, No. 1, pp. 119–166, http://dx.doi.org/10.2138/rmg.2022.88.02
Hughes E.B. (2019) Micro-World: Curved banding in flame-fusion synthetic sapphires. *G&G*, Vol. 55, No. 2, pp. 264–265.
Hughes E.B., Perkins R. (2019) Madagascar sapphire: Low-temperature heat treatment experiments. *G&G*, Vol. 55, No. 2, pp. 184–197, http://dx.doi.org/10.5741/GEMS.55.2.184
Hughes E.B., Vertriest W. (2022) A canary in the ruby mine: Low-temperature heat treatment experiments on Burmese ruby. *G&G*, Vol. 58, No. 4. pp. 400–423, http://dx.doi.org/10.5741/GEMS.58.4.400
Hughes R.W., Emmett J.L. (2005) Heat seeker | UV fluorescence as a gemological tool. LotusGemology.com, https://www.lotusgemology.com/resources/articles/156-heat-seeker-uv-fluorescence-as-a-gemological-tool
Hughes R.W., Manorotkul W., Hughes E.B. (2017) *Ruby & Sapphire: A Gemologist's Guide*; RWH Publishing/Lotus Publishing: Bangkok, 732 pp.
Iwahashi Y., Akamatsu S. (1994) Porphyrin pigment in black-lip pearls and its application to pearl identification. *Fisheries Science*, Vol. 60, No. 1, pp. 69–71, http://dx.doi.org/10.2331/fishsci.60.69
Johnson P., Moe K.S., Persaud S., Odake S., Kazuchits N.M., Zaitsev A.M. (2023) Spectroscopic characterization of yellow *gem* quality CVD diamond. *Diamond and Related Materials*, Vol. 140, Part B, article no. 110505, http://dx.doi.org/10.1016/j.diamond.2023.110505
Ju M.J., Lee S.J., Kim Y., Shin J.G., Kim H.Y., Lim Y., Yasuno Y., Lee B.H. (2011) Multimodal analysis of pearls and pearl treatments by using optical coherence tomography and fluorescence spectroscopy. *Optics Express*, Vol. 19., No. 7, pp. 6420–6432, http://dx.doi.org/10.1364/OE.19.006420
Kanda H., Akaishi M., Setaka N., Yamaoka S., Fukunaga O. (1980) Surface structures of synthetic diamonds. *Journal of Materials Science*, Vol. 15, No. 11, pp. 2743–2748, http://dx.doi.org/10.1007/BF00550541
Kanda H., Ohsawa T., Fukunaga O., Sunagawa I. (1989) Effect of solvent metals upon the morphology of synthetic diamonds. *Journal of Crystal Growth*, Vol. 94, No. 1, pp. 115–124, http://dx.doi.org/10.1016/0022-0248(89)90610-6
Kiefert L., McLaurin Moreno D., Arizmendi E., Hänni H.A., Elen S. (2004) Cultured pearls from the Gulf of California, Mexico. *G&G*, Vol. 40, No. 1, pp. 26–38, http://dx.doi.org/10.5741/GEMS.40.1.26
Kiflawi I., Kanda H., Lawson S.C. (2002) The effect of the growth rate on the concentration of nitrogen and transition metal impurities in HPHT synthetic diamonds. *Diamond and Related Materials*, Vol. 11, No. 2, pp. 204–211, http://dx.doi.org/10.1016/S0925-9635(01)00569-6
Kunz G.F., Baskerville C. (1903) The action of radium, roentgen rays and ultra-violet light on minerals and gems. *Science*, Vol. 18, No. 468, pp. 769–783, http://dx.doi.org/10.1126/science.18.468.769
Lai L.T.-A. (2016) Gem News International: Application of the DiamondView in separating impregnated jadeite. *G&G*, Vol. 52, No. 3, pp. 327–328.
——— (2018a) Gem News International: Separating glass-filled rubies using the DiamondView. *G&G*, Vol. 54, No. 2, pp. 458–459.
——— (2018b) Gem News International: Emeralds filled with epoxy resin: DiamondView observations. *G&G*, Vol. 54, No. 4, pp. 250–251.
——— (2018c) Gem News International: Strong fluorescence in B-jade impregnated with wax. *G&G*, Vol. 54, No. 2, pp. 251–252.
Lai M.Y., Hardman M.F., Eaton-Magaña S., Breeding C.M., Schwartz V.A., Collins A.T. (2024) Spectroscopic characterization of diamonds colored by the 480 nm absorption band. *Diamond and Related Materials*, Vol. 142, article no. 110825, http://dx.doi.org/10.1016/j.diamond.2024.110825
Laidlaw F.H.J., Beanland R., Fisher D., Diggle P.L. (2020) Point defects and interstitial climb of 90° partial dislocations in brown type IIa natural diamond. *Acta Materialia*, Vol. 201, pp. 494–503, http://dx.doi.org/10.1016/j.actamat.2020.10.033
Laidlaw F.H.J., Diggle P.L., Breeze B.G., Dale M.W., Fisher D., Beanland R. (2021) Spatial distribution of defects in a plastically deformed natural brown diamond. *Diamond and Related Materials*, Vol. 117, article no. 108465, http://dx.doi.org/10.1016/j.diamond.2021.108465
Lan Y., Lu T., Zhang C., Liang R., Ding T., Chen H., Ke J., Bi L. (2016) Development of a new multi-spectral induced luminescence imaging system (GV5000) and its application in screening melee-sized near-colorless synthetic diamonds and natural diamonds. *Rock and Mineral Analysis*, Vol. 35, No. 5, pp. 505–512 (in Chinese with English abstract).
Lang A.R. (1974) On the growth-sectorial dependence of defects in natural diamonds. *Proceedings of the Royal Society of London. Series A*, Vol. 340, No. 1621, pp. 233–248, http://dx.doi.org/10.1098/rspa.1974.0150
——— (1979) Internal structure. In J.E. Field, Ed., *The Properties of Diamond*, Academic Press, London, pp. 425–469.
Law B.P.L., Wang W. (2016) Lab Notes: CVD synthetic diamond over 5 carats identified. *G&G*, Vol. 52, No. 4, pp. 414–416.
Lawson S.C., Kanda H., Watanabe K., Kiflawi I., Sato Y., Collins A.T. (1996) Spectroscopic study of cobalt-related optical centers in synthetic diamond. *Journal of Applied Physics*, Vol. 79, No. 8, pp. 4348–4357, http://dx.doi.org/10.1063/1.361744
Lecoq de Boisbaudran P.E. (1887) Sur la fluorescence rouge de l'alumine. *Comptes Rendus Hebdomadaires des Séances de l'Académie des Sciences*, Vol. 104, pp. 330–334.
Lu R. (2012) Color origin of lavender jadeite: An alternative approach. *G&G*, Vol. 48, No. 4, pp. 273–283, http://dx.doi.org/10.5741/GEMS.48.4.273
Luo Y., Breeding C.M. (2013) Fluorescence produced by optical defects in diamond: Measurement, characterization, and challenges. *G&G*, Vol. 49, No. 2, pp. 82–97, http://dx.doi.org/10.5741/GEMS.49.2.82
Martineau P.M., Lawson S.C., Taylor A.J., Quinn S.J., Evans D.J.F., Crowder M.J. (2004) Identification of synthetic diamond grown using chemical vapor deposition (CVD). *G&G*, Vol. 40, No. 1, pp. 2–25, http://dx.doi.org/10.5741/GEMS.40.1.2
Martineau P., Gaukroger M., Khan R., Evans D. (2009) Effect of steps on dislocations in CVD diamond grown on {001} substrates. *physica status solidi c*, Vol. 6, No. 8, pp. 1953–1957, http://dx.doi.org/10.1002/pssc.200881465
Mauthner M. (2020) Fluorescence in gems. *Rocks & Minerals*, Vol. 96, No. 1, pp. 38–43, http://dx.doi.org/10.1080/00357529.2021.1827909
Mawe J. (1813) *A Treatise on Diamonds and Precious Stones: Including Their History – Natural and Commercial. To which is Added, Some Account of the Best Methods of Cutting and Polishing Them*. Longman, Hurst, Rees, Orme, and Brown, London.
McGuinness C.D., Wassell A.M., Lanigan P.M.P., Lynch S.A.

(2020) Separation of natural from laboratory-grown diamond using time-gated luminescence imaging. *G&G*, Vol. 56, No. 2, pp. 220–229, http://dx.doi.org/10.5741/GEMS.56.2.220
Meng Y.F., Yan C.S., Lai J., Krasnicki S., Shu H., Yu T., Liang Q., Mao H.K., Hemley R.J. (2008) Enhanced optical properties of chemical vapor deposited single crystal diamond by low-pressure/high-temperature annealing. *Proceedings of the National Academy of Sciences*, Vol. 105, No. 46, pp. 17620–17625, http://dx.doi.org/10.1073/pnas.0808230105
Miyoshi T. (1992) Effect of light irradiation on fluorescence and optical reflectance of pearls. *Technology Reports of Yamaguchi University*, Vol. 5, No. 1, pp. 23–30.
Miyoshi T., Matsuda Y., Komatsu H. (1987) Fluorescence from pearls and shells of black lip oyster, *Pinctada margaritifera*, and its contribution to the distinction of mother oysters used in pearl culture. *Japanese Journal of Applied Physics*, Vol. 26, No. 7, pp. 1069–1072.
Moe K.S., Johnson P. (2007) Lab Notes: Blue diamonds showing multiple colors of phosphorescence. *G&G*, Vol. 43, No. 1, pp. 47–48.
Moe K.S., D'Haenens-Johansson U., Wang W. (2015) Lab Notes: Irradiated green-blue CVD synthetic diamonds. *G&G*, Vol. 51, No. 3, pp. 320–321.
Moe K.S., Johnson P., D'Haenens-Johansson U., Wang W. (2017) Lab Notes: A synthetic diamond overgrowth on a natural diamond. *G&G*, Vol. 53, No. 2, pp. 237–239.
Moore M., Lang A.R. (1972) On the internal structure of natural diamonds of cubic habit. *Philosophical Magazine*, Vol. 26, No. 6, pp. 1313–1325, http://dx.doi.org/10.1080/14786437208220345
Moses T.M., Reinitz I.M., Johnson M.L., King J.M., Shigley J.E. (1997) A contribution to understanding the effect of blue fluorescence on the appearance of diamonds. *G&G*, Vol. 33, No. 4, pp. 244–259, http://dx.doi.org/10.5741/GEMS.33.4.244
Nasdala L., Fritsch E. (2024) Luminescence: The "cold glow" of minerals. *Elements*, Vol. 20, No. 5, pp. 287–292, http://dx.doi.org/10.2138/gselements.20.5.287
Nasdala L., Grambole D., Wildner M., Gigler A.M., Hainschwang T., Zaitsev A.M., Harris J.W., Milledge J., Schulze D.J., Hofmeister W., Balmer W.A. (2013) Radio-colouration of diamond: A spectroscopic study. *Contributions to Mineralogy and Petrology*, Vol. 165, No. 5, pp. 843–861, http://dx.doi.org/10.1007/s00410-012-0838-1
Nichols E.L., Howes H.L. (1929) The transformation spectrum of the ruby. *Proceedings of the National Academy of Sciences*, Vol. 15, No. 2, pp. 139–146, http://dx.doi.org/10.1073/pnas.15.2.139
Notari F., Grobon C., Fritsch E. (2002) Observation des émeraudes traitées en luminescence UVISIO® Quelle mention attribuer aux émeraudes après suppression des résines synthétiques de leurs fissures? *Revue de Gemmologie AFG*, Vol. 144, pp. 27–31 (in French).
Palyanov Y.N., Kupriyanov I.N., Khokhryakov A.F., Ralchenko V.G. (2015) Crystal growth of diamond. In P. Rudolph, Ed., *Handbook of Crystal Growth*, Elsevier, Boston, pp. 671–713.
Pearson G. (2011) Review of ultraviolet sources for gem fluorescence and testing. *Journal of Gemmology*, Vol. 32, No. 5-8, pp. 211–222.
Ponahlo J. (2000) Cathodoluminescence as a tool for gemstone identification. In M. Pagel et al., Eds., *Cathodoluminescence in Geosciences*, Springer, Berlin, pp. 479–500.
Robinson A. (2018) Irradiated HPHT-grown diamonds might escape detection as synthetics, says lab. *IDEX Online*, http://www.idexonline.com/FullArticle?Id=43871
Ruan J., Kobashi K., Choyke W.J. (1992) On the "band-A" emission and boron related luminescence in diamond. *Applied Physics Letters*, Vol. 60, No. 25, pp. 3138–3140, http://dx.doi.org/10.1063/1.106748
Satoh S., Sumiya H., Tsuji K., Yazu S. (1990) Differences in nitrogen concentration and aggregation among {111} and {100} growth sectors of large synthetic diamonds. In S. Saito, Eds., *Science and Technology of New Diamond*, KTK Scientific Publishers/Terra Scientific Publishing Co., Tokyo, pp. 351–355.
Schulze D.J., Nasdala L. (2016) Unusual paired pattern of radiohaloes on a diamond crystal from Guaniamo (Venezuela). *Lithos*, Vol. 265, pp. 177–181, http://dx.doi.org/10.1016/j.lithos.2016.09.024
Shen A., Eaton-Magaña S. (2011) Lab Notes: Type IIb diamond with long phosphorescence, *G&G*, Vol. 47, No. 4, pp. 308–315.
Shi L., Wang Y., Liu X., Mao J. (2018) Component analysis and identification of black Tahitian cultured pearls from the oyster *Pinctada margaritifera* using spectroscopic techniques. *Journal of Applied Spectroscopy*, Vol. 85, No. 1, pp. 98–102, http://dx.doi.org/10.1007/s10812-018-0618-4
Shigley J.E., Breeding C.M. (2013) Optical defects in diamond: A quick reference chart. *G&G*, Vol. 49, No. 2, pp. 107–111, http://dx.doi.org/10.5741/GEMS.49.2.107
Shigley J.E., Breeding C.M., Shen A.H.T. (2004a) An updated chart on the characteristics of HPHT-grown synthetic diamonds. *G&G*, Vol. 40, No. 4, pp. 303–313, http://dx.doi.org/10.5741/GEMS.40.4.303
Shigley J.E., McClure S.F., Breeding C.M., Shen A.H.T., Muhlmeister S.M. (2004b) Lab-grown colored diamonds from Chatham Created Gems. *G&G*, Vol. 40, No. 2, pp. 128–145, http://dx.doi.org/10.5741/GEMS.40.2.128
Smit K.V., Shirey S.B. (2020) Diamonds from the Deep: Diamonds are not forever! Diamond dissolution. *G&G*, Vol. 56, No. 1, pp. 148–155.
Smit K.V., Myagkaya E., Persaud S., Wang W. (2018) Black diamonds from Marange (Zimbabwe): A result of natural irradiation and graphite inclusions. *G&G*, Vol. 54, No. 2, pp. 132–148, http://dx.doi.org/10.5741/GEMS.54.2.132
Smith E.M. (2023) Diamond Reflections: Plastic deformation: How and why are most diamonds slightly distorted? *G&G*, Vol. 59, No. 1, pp. 94–99.
Smith E.M., Shirey S.B., Nestola F., Bullock E.S., Wang J., Richardson S.H., Wang W. (2016) Large gem diamonds from metallic liquid in Earth's deep mantle. *Science*, Vol. 354, No. 6318, pp. 1403–1405, http://dx.doi.org/10.1126/science.aal1303
Smith E.M., Shirey S.B., Wang W. (2017) The very deep origin of the world's biggest diamonds. *G&G*, Vol. 53, No. 4, pp. 388–403, http://dx.doi.org/10.5741/GEMS.53.4.388
Sohrabi S., Anjomani N. (2022) Lab Notes: Hydrothermal synthetic ruby. *G&G*, Vol. 58, No. 1, pp. 57–58.
Stokes G.G. (1852) On the change of refrangibility of light. *Philosophical Transactions of the Royal Society of London*, Vol. 142, pp. 463–562, http://dx.doi.org/10.1098/rstl.1852.0022
Strong H.M., Chrenko R.M. (1971) Further studies on diamond growth rates and physical properties of laboratory-made diamond. *Journal of Physical Chemistry*, Vol. 75, No. 12, pp. 1838–1843, http://dx.doi.org/10.1021/j100681a014
Sturman N., Homkrajae A., Manustrong A., Somsa-ard N. (2014) Observations on pearls reportedly from the Pinnidae family (pen pearls). *G&G*, Vol. 50, No. 3, pp. 202–215, http://dx.doi.org/10.5741/GEMS.50.3.202
Sturman N., Otter L.M., Homkrajae A., Manustrong A., Nilpetploy N., Lawanwong K., Kessrapong P., Jochum K.P., Stoll B., Götz H., Jacob D.E. (2019) A pearl identification challenge. *G&G*, Vol. 55, No. 2, pp. 229–243, http://dx.doi.org/10.5741/GEMS.55.2.229
Sumiya H., Toda N., Satoh S. (2002) Growth rate of high-quality large diamond crystals. *Journal of Crystal Growth*, Vol. 237–239, pp. 1281–1285, http://dx.doi.org/10.1016/S0022-0248(01)02145-5
Sunagawa I. (1984) Morphology of natural and synthetic diamond crystals. In I. Sunagawa, Ed., *Materials Science of the Earth's Interior*, Terra Scientific Publishing Co., Tokyo, pp. 303–330.
——— (1995) The distinction of natural from synthetic diamond. *Journal of Gemmology*, Vol. 24, No. 7, pp. 485–499.
Suzuki S., Lang A.R. (1976) Internal structures of natural diamonds revealing mixed-habit growth. In P. Daniel, Ed., *Diamond Re-*

search, Industrial Diamond Information Bureau, Ascot, UK, pp. 39–47.
Tam K.W., Poon T.P.Y. (2023) Lab Notes: CVD diamond over 34 carats. *G&G*, Vol. 59, No. 2, pp. 213–214.
Tang S., Su J., Lu T., Ma Y., Ke J., Song Z., Zhang J., Liu H. (2018) A thick overgrowth of CVD synthetic diamond on a natural diamond. *Journal of Gemmology*, Vol. 36, No. 2, pp. 134–141.
Thomaz M.F., Davies G. (1978) The decay time of N3 luminescence in natural diamond. *Proceedings of the Royal Society of London. Series A*. Vol. 362, No. 1710, pp. 405–419, http://dx.doi.org/10.1098/rspa.1978.0141
Tsai T.-H. (2021) Multi-excitation fluorescence imaging for identifying clarity enhancement in gemstones. *Proceedings SPIE 11815, Novel Optical Systems, Methods, and Applications XXIV*, article no. 1181505, http://dx.doi.org/10.1117/12.2592939
Tsai T.-H., D'Haenens-Johansson U.F.S. (2021) Rapid gemstone screening and identification using fluorescence spectroscopy. *Applied Optics*, Vol. 60, No. 12, pp. 3412–3421, http://dx.doi.org/10.1364/AO.419885
Tsai T.-H., Zhou C. (2021) Rapid detection of color-treated pearls and separation of pearl types using fluorescence analysis. *Applied Optics*, Vol. 60, No. 20, pp. 5837–5845, http://dx.doi.org/10.1364/AO.427203
Tsai T.-H., D'Haenens-Johansson U.F.S., Smith T., Zhou C., Xu W. (2024) Multi-excitation photoluminescence spectroscopy system for gemstone analysis. *Optics Express*, Vol. 32, No. 14, pp. 24839–24855, http://dx.doi.org/10.1364/OE.525832
Wang M., Shi G., Yuan J.C.C., Han W., Bai Q. (2018) Spectroscopic characteristics of treated-color natural diamonds. *Journal of Spectroscopy*, Vol. 2018, article no. 81532941, http://dx.doi.org/10.1155/2018/8153941
Wang W., Scarratt K., Hyatt A., Shen A.H.-T., Hall M. (2006) Identification of "chocolate pearls" treated by Ballerina Pearl Co. *G&G*, Vol. 42, No. 4, pp. 222–235, http://dx.doi.org/10.5741/GEMS.42.4.222
Wang W., Hall M.S., Moe K.S., Tower J., Moses T.M. (2007) Latest-generation CVD-grown synthetic diamonds from Apollo Diamond Inc. *G&G*, Vol. 43, No. 4, pp. 294–312, http://dx.doi.org/10.5741/GEMS.43.4.294
Wang W., Doering P., Tower J., Lu R., Eaton-Magaña S., Johnson P., Emerson E., Moses T.M. (2010) Strongly colored pink CVD lab-grown diamonds. *G&G*, Vol. 46, No. 1, pp. 4–17, http://dx.doi.org/10.5741/GEMS.46.1.4
Wang W., D'Haenens-Johansson U.F.S., Johnson P., Moe K.S., Emerson E., Newton M.E., Moses T.M. (2012) CVD synthetic diamond from Gemesis Corp. *G&G*, Vol. 48, No. 2, pp. 80–97, http://dx.doi.org/10.5741/GEMS.48.2.80
Wassell A.M., McGuinness C.D., Hodges C., Lanigan P.M.P., Fisher D., Martineau P.M., Newton M.E., Lynch S.A. (2018) Anomalous green luminescent properties in CVD synthetic diamonds. *physica status solidi (a)*, Vol. 215, No. 22, article no. 1800292, http://dx.doi.org/10.1002/pssa.201800292
Watanabe K., Lawson S.C., Isoya J., Kanda H., Sato Y. (1997) Phosphorescence in high-pressure synthetic diamond. *Diamond and Related Materials*, Vol. 6, No. 1, pp. 99–106, http://dx.doi.org/10.1016/S0925-9635(96)00764-9
Waychunas G.A. (2014) Luminescence spectroscopy. *Reviews in Mineralogy and Geochemistry*, Vol. 78, No. 1, pp. 175–217, http://dx.doi.org/10.2138/rmg.2014.78.5
Waychunas G., Kempe U. (2024) Activators in minerals and the role of electronic defects. *Elements*, Vol. 20, No. 5, pp. 293–298, http://dx.doi.org/10.2138/gselements.20.5.293
Webster R. (1975) *Gems: Their Sources, Descriptions and Identification*, 3rd ed. Archon Books, Butterworth & Co., London.
——— (1983) *Gems: Their Sources, Descriptions and Identification*, 4th ed. Butterworths, London.
Welbourn C.M., Rooney M.-L.T., Evans D.J.F. (1989) A study of diamonds of cube and cube-related shape from the Jwaneng mine. *Journal of Crystal Growth*, Vol. 94, No. 1, pp. 229–252, http://dx.doi.org/10.1016/0022-0248(89)90622-2
Welbourn C.M., Cooper M., Spear P.M. (1996) De Beers natural versus synthetic diamond verification instruments. *G&G*, Vol. 32, No. 3, pp. 156–169, http://dx.doi.org/10.5741/GEMS.32.3.156
Willems B., Martineau P.M., Fisher D., Van Royen J., Van Tendeloo G. (2006) Dislocation distributions in brown diamond. *physica status solidi (a)*, Vol. 203, No, 12, pp. 3076–3080, http://dx.doi.org/10.1002/pssa.200671129
Williams B. (2007) Technology update—Ultraviolet light. *Gem Market News*, Vol. 26, pp. 8–11.
Wong W.C., McClure D.C., Basun S.A., Kokta M.R. (1995a) Charge-exchange processes in titanium-doped sapphire crystals. I. Charge-exchange energies and titanium-bound excitons. *Physical Review B*, Vol. 51, No. 9, pp. 5682–5692, http://dx.doi.org/10.1103/PhysRevB.51.5682
——— (1995b) Charge-exchange processes in titanium-doped sapphire crystals. II. Charge-transfer transition states, carrier trapping, and detrapping. *Physical Review B*, Vol. 51, No. 9, pp. 5693–5698, http://dx.doi.org/10.1103/PhysRevB.51.5693
van Wyk J.A., Loubser J.H.N. (1993) ENDOR of the P2 centre in type-Ia diamonds. *Journal of Physics: Condensed Matter*, Vol. 5, No. 18, pp. 3019–3026, http://dx.doi.org/10.1088/0953-8984/5/18/024
Yelisseyev A., Kanda H. (2007) Optical centers related to 3d transition metals in diamond. *New Diamond and Frontier Carbon Technology*, Vol. 17, pp. 127–178.
Yu H., Clarke D.R. (2002) Effect of codoping on the R-line luminescence of Cr^{3+}-doped alumina. *Journal of the American Ceramic Society*, Vol. 85, No. 8, pp. 1966–1970, http://dx.doi.org/10.1111/j.1151-2916.2002.tb00389.x
Zaitsev A.M. (2001) *Optical Properties of Diamond: A Data Handbook*. Springer, Berlin.
Zandi F. (2021) Lab Notes: Lead glass-filled laboratory-grown ruby. *G&G*, Vol. 57, No. 1, pp. 61–62.
Zhang J., Lu T., Chen H. (2013) Characteristics of coated jadeite jade. *G&G*, Vol. 49, No. 4, pp. 246–251, http://dx.doi.org/10.5741/GEMS.49.4.246
Zhang Z., Shen A. (2023) Fluorescence and phosphorescence spectroscopies and their applications in gem characterization. *Minerals*, Vol. 13, No. 5, article no. 626, http://dx.doi.org/10.3390/min13050626
Zhao J., Green B.L., Breeze B.G., Newton M.E. (2023) Phosphorescence and donor-acceptor pair recombination in laboratory-grown diamond. *Physical Review B*, Vol. 108, No. 16, article no. 165203, http://dx.doi.org/10.1103/PhysRevB.108.165203
Zhou C., Homkrajae A., Ho J.W.Y., Hyatt A., Sturman N. (2012) Update on the identification of dye treatment in yellow or "golden" cultured pearls. *G&G*, Vol. 48, No. 4, pp. 284–291, http://dx.doi.org/10.5741/GEMS.48.4.284
Zhou C., Ho J.W.Y., Chan S., Zhou J.Y., Wong S.D., Moe K.S. (2016) Identification of "pistachio" colored pearls treated by Ballerina Pearl Co. *G&G*, Vol. 52, No. 1, pp. 50–59, http://dx.doi.org/10.5741/GEMS.52.1.50
Zhou C., Tsai T.-H., Sturman N., Nilpetploy N., Manustrong A., Lawanwong K. (2020) Optical whitening and brightening of pearls: A fluorescence spectroscopy study. *G&G*, Vol. 56, No. 2, pp. 258–265, http://dx.doi.org/10.5741/GEMS.56.2.258
Zhou C., Ho J.W.Y., Shih S.C., Tsai T.-H., Sun Z., Persaud S., Qi L.-J. (2021) Detection of color treatment and optical brightening in Chinese freshwater "Edison" pearls. *G&G*, Vol. 57, No. 2, pp. 124–134, http://dx.doi.org/10.5741/GEMS.57.2.124